https://doi.org/10.5194/egusphere-2025-2905
Preprint. Discussion started: 27 June 2025

Severe reduction of carbon, alkalinity and nutrient fluxes in the southern Baltic Sea caused by dragging of trawl ropes across the seafloor

Pankan Linsy [1], Stefan Sommer[1], Jens Kallmeyer[2], Simone Bernsee[2], Florian Scholz[3], Habeeb Thanveer Kalapurakkal[1a], Andrew W. Dale[1]

[1] GEOMAR Helmholtz Centre for Ocean Research Kiel, Wischhofstraße 1–3, 24148 Kiel, Germany

[2]GFZ Helmholtz Centre for Geosciences, Telegrafenberg, 14473 Potsdam, Germany

[3] Institute for Geology, Center for Earth System Research and Sustainability, Universität Hamburg, Hamburg, Germany.

[a] Now at: Alfred Wegener Institute Helmholtz Centre for Polar and Marine Research, 27570 Bremerhaven, Germany

Correspondence to: Pankan Linsy (linsyp@geomar.de)

Abstract

Bottom trawling represents a substantial anthropogenic disturbance, significantly disrupting seafloor integrity and altering oceanic carbon storage. In this study, we conducted a benthic trawling experiment on organic-rich muddy sediments in the Mecklenburger Bight, southern Baltic Sea, employing an otter trawl. Multiple trawl tracks were made to assess the temporal impact of bottom fishing on the benthic ecosystem over time scales ranging from days to weeks. Focus was on the wide area where the net footrope was dragged between the otter boards, rather than on much smaller area impacted by the trawl doors. This study constitutes the first comprehensive investigation to systematically monitor the effects of bottom trawling on benthic oxygen, carbon, alkalinity and nutrient fluxes using autonomous in situ lander measurements. Seafloor observations revealed a profound impact of trawling on seafloor morphology. Flux measurements, coupled with sediment data, indicated reductions in benthic fluxes of O_2, dissolved inorganic carbon (DIC), total alkalinity (TA), and nutrients within trawled areas compared to control sites. Additionally, observed variations in organic carbon remineralization rates suggest that bottom trawling suppresses benthic respiration by disrupting key biogeochemical processes. Fluxes of O_2, DIC, and TA had not returned to baseline levels by the conclusion of the 16-day observation period, indicating prolonged disturbance effects although the reduction in O_2 fluxes was more caused by decreasing bottom water O_2 levels over the study period. Despite substantial alterations to the benthic ecosystem, modeling suggests that the reduction in benthic DIC and TA fluxes exerts only a minor influence on CO_2 release to the atmosphere compared to the much larger impact of pyrite oxidation in resuspended sediment.

1. Introduction

Bottom trawling is one of the major anthropogenic activities that significantly affect the marine environment (Depestele et al., 2019; Hiddink et al., 2006; Oberle et al., 2016b; Olsgard et al., 2008; Pusceddu et al., 2014). Trawling involves catching benthic and demersal fish by towing nets along the seafloor using various devices. Bottom trawling gear can penetrate the seafloor and dislocate the sediment to varying depths depending on the sediment type and gear used (Martín et al., 2014). Approximately 4.9 million km^2 or 1.3% of the global ocean is estimated to be trawled each year (Sala et al., 2021). The impacts of bottom trawling include the alteration of seabed morphology through the scraping, ploughing, and resuspension of surface sediments (Bruns et al., 2023; Oberle et al., 2016b). These processes ultimately disrupt benthic biogeochemical cycles (Allen and Clarke, 2007; Bradshaw et al., 2021; Bruns et al., 2023; Hale et al., 2017; Morys et al., 2021; Sciberras et al., 2016; Tiano et al., 2019; van de Velde et al., 2018). Additionally, bottom trawling has been shown to significantly reduce benthic fauna biomass (Bergman, 2000; Bergman and Meesters, 2020; Tiano et al., 2022) and, ultimately, change benthic community structures (Bradshaw et al., 2024; Kaiser et al., 2002; Pusceddu et al., 2014).

https://doi.org/10.5194/egusphere-2025-2905
Preprint. Discussion started: 27 June 2025

The seafloor disturbance caused by trawling has been argued to disrupt oceanic carbon sequestration (Atwood et al., 2024; Epstein et al., 2022; Hiddink et al., 2023; Sala et al., 2021; Zhang et al., 2024) as marine sediments serve as a critical reservoir for long-term carbon storage (Burdige, 2007; LaRowe et al., 2020). The study by Sala et al., (2021) suggests that seafloor disturbances caused by trawling and dredging result in the annual release of 0.58–1.47 Pg of CO_2, largely due to increased remineralization of particulate organic carbon (POC). Atwood et al. (2024) estimated that 50–60% of the CO_2 released due to trawling is emitted into the atmosphere over a decade, accounting for approximately 0.34–0.37 Pg CO_2 per year globally. However, a subsequent metadata analysis by Epstein et al., (2022) yielded mixed findings on the impact of trawling on POC stock, revealing no significant effect in 61% of the 49 studies analyzed. Among the remaining studies, 29% reported decreased POC levels associated with fishing activities, while 10% observed an increase in POC. These results indicate that the impact of bottom trawling is site-specific and probably influenced by factors such as trawling frequency, type of fishing gear, local lithology, and towing intensity (De Borger et al., 2021; Depestele et al., 2019; Oberle et al., 2016a; Tiano et al., 2019). Thus, site-specific studies are necessary for studying the impact of bottom trawling in any given region (Stephens and McConnaughey, 2024).

Bottom fishing is carried out over large swathes of the Baltic Sea (HELCOM, 2018), and approximately 36% of the seafloor in the southwestern Baltic Sea is affected (Díaz-Mendoza et al., 2025). A study by Van Denderen et al. (2020) revealed that trawling, together with bottom water hypoxia, has led to a 50 % reduction in benthic biomass in 14% of the Baltic Sea region. The impact of bottom trawling on the benthos in the Baltic Sea has been the subject of numerous studies (Bradshaw et al., 2021, 2024; Bunke et al., 2019; Corell et al., 2023; Morys et al., 2021; Porz et al., 2023; Rooze et al., 2024; Schönke et al., 2022), but relatively few have examined the impact on benthic biogeochemistry (Bradshaw et al., 2021, 2024; Morys et al., 2021; Rooze et al., 2024; Tiano et al., 2024). Morys et al. (2021) conducted a controlled benthic dredging experiment in previously untrawled regions of the Baltic Sea. The experiment simulated the sediment disturbance caused by trawl gears by removing the surface sediment, allowing for a comparative analysis of geochemical characteristics with an adjacent pristine area. Immediate post-disturbance observations indicated alterations in benthic nutrient fluxes and porewater profiles. Bradshaw et al., (2021) conducted a controlled field experiment in muddy sediments of the Baltic Proper using a commercial otter trawl to quantify the physical and biogeochemical impacts of bottom trawling. Their findings indicated a reduction in oxygen penetration depth into the seafloor as well as altered nutrient and oxygen fluxes across the sediment-water interface. The trawl track persisted for at least 18 months, which suggests that sediment biogeochemistry may not fully recover in areas with frequent bottom trawling. However, as a single-track experiment, these findings may not fully represent the cumulative impacts of trawling, particularly in areas where bottom trawling occurs intensively more than 10 times per year (HELCOM, 2018).

When examining the impact of trawling activities on the oceanic carbon pool, it is also crucial to consider the effects of trawling on sedimentary total alkalinity (TA) and dissolved inorganic carbon (DIC) fluxes rather than solely focusing on organic carbon remineralization. Sediment-water reactions influence the ocean's buffering capacity, thereby affecting its ability to take up CO_2 from the atmosphere (Zeebe and Wolf-Gladrow, 2001). In the continental shelf ecosystem, in addition to the burial of organic carbon, benthic alkalinity production plays a key role in net carbon sequestration (Van Dam et al., 2022). The shallowness of coastal seas further permits a close interaction between sediments and the atmosphere (Brenner et al., 2016; Burt et al., 2016). Several processes control alkalinity generation in sediments and fluxes to the water column, such as mineral formation and dissolution, denitrification, pyrite formation and burial, and reverse weathering (Krumins et al., 2013; Middelburg et al., 2020). Experimental and model studies have shown that trawling-induced resuspension reduces the capacity of the Baltic Sea to remove atmospheric CO_2 by decreasing alkalinity, mainly through the oxidation of pyrite (Kalapurakkal et al., 2025). The field observations conducted to date have not specifically investigated the impact of bottom trawling on alkalinity fluxes. Therefore, additional field-based investigations are essential to comprehensively understand the influence of bottom trawling on the broader carbon cycle in addition to the associated biogeochemical upheavals at the sediment surface.

As a step toward addressing these critical knowledge gaps, we conducted a benthic trawling experiment in Mecklenburger Bight within the German Exclusive Economic Zone (EEZ) of the Baltic Sea. An otter trawl was deployed to create multiple trawl tracks. Subsequently, dissolved oxygen, DIC, TA, and nutrient fluxes were measured in situ using benthic landers to assess the effect of trawling on sediment regeneration rates, as well as a detailed survey of sediment biogeochemical parameters in recovered sediment cores. Due to low probability of deploying large gears directly on the trawl marks gouged out of by the otter boards, we chose to target instead the much wider net area between the trawl boards (termed the 'net zone'). In addition to the benthic working program, we carried out seafloor imaging to observe the degree of disturbance and redistribution of sediments possibly affecting benthic communities. The major aim of the fieldwork was to determine the direct effects of bottom trawling on the benthic ecosystem on time scales of days to weeks and the regeneration capacity of sediment biogeochemistry. We also explore how changes to benthic TA and DIC fluxes impact air-sea CO_2 exchange. Our

https://doi.org/10.5194/egusphere-2025-2905
Preprint. Discussion started: 27 June 2025

results provide novel insights into trawling-induced alterations in benthic biogeochemical processing in coastal environments.

2. Materials and Methods

2.1 Study area and experimental strategy

The research cruise AL616 on RV Alkor was undertaken from 18 July to 9 August 2024 in the German EEZ of the Baltic Sea (Sommer et al., 2025). The cruise was embedded in a larger campaign further addressing effects of trawling on different size classes of benthic communities (macrobenthos, meiofauna, protozoans and bacteria/archaea), including sedimentological investigations. Aside from RV Alkor, four research vessels participated in this trawling experiment. On RV Elisabeth Mann Borgese (cruise EMB 345), sediments were sampled for biological analyses. Scientists on the RV Clupea (cruise #389) carried out the trawling and investigated the effects of trawling on fish populations. The width of the net impacted by scraping of the surface sediment by the footrope and rollers was 60 m. SCUBA diving operations were performed using the RV Limanda, and the small tender Klashahn was used to survey the seabed using hydroacoustics.

The working area was located in the Mecklenburger Bight (southwestern Baltic Sea) 5 km offshore the town of Kühlungsborn at water depths of ~23 m (Fig. 1). It comprises the High-Impact (HI) area with dimensions of 1000 x 200 m that was trawled several times in an east – west direction on 20 July 2024. A Control area (CL) of similar size where no trawling was performed was located west of the HI area. The sediments across the working area were fine-grained muds.

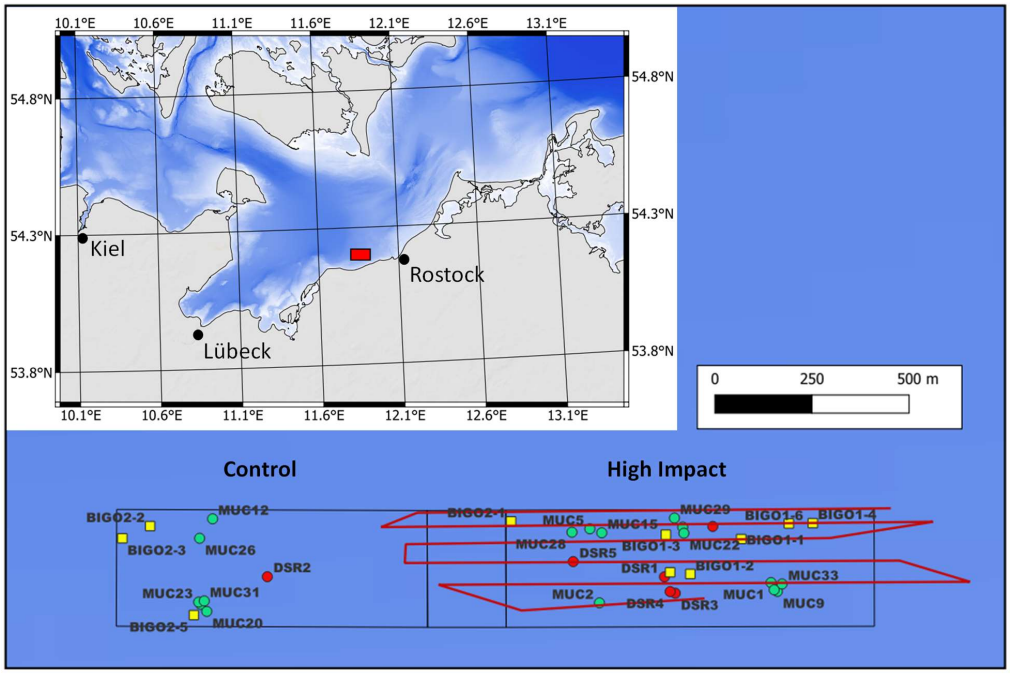

Figure 1: Trawling area indicating BIGO (yellow squares), MUC (green circles), and deep-sea rover (DSR) (red circles) deployment sites. Red lines indicate trawl tracks. The inset shows the sampling area (red box) in the western Baltic.

2.2 Water and sediment sampling

https://doi.org/10.5194/egusphere-2025-2905
Preprint. Discussion started: 27 June 2025

A Sea-Bird Scientific CTD (SBE 9) equipped with a 12-Niskin bottle water sampling rosette was utilized for in situ measurements of salinity, temperature, depth and chlorophyll-a and for retrieving water samples. Data acquisition was performed using Sea-Bird Seasave software (v7.26.7). A total of seven CTD casts were conducted, with three deployments in the CL are and four in the HI area. Water samples for dissolved oxygen measurement were immediately analyzed onboard using the Winkler method. Samples for nutrient analysis were collected and analyzed onboard.

Sediment samples were collected using a multiple-corer (MUC) with 6 and 11 deployments in the CL and HI areas, respectively (Table S1). The MUC was equipped with seven Perspex liners, each 60 cm in length and 10 cm in internal diameter. The MUC was lowered toward the seafloor at a speed of 0.3 m s^{-1} in every deployment. Upon reaching the seafloor, lead weights applied gravitational force to drive the liners into the sediment, with a maximum penetration depth of 35 cm. Upon retrieval, all cores were moved to a cooling laboratory maintained at 10°C, which approximates the bottom water temperature at the sampling sites. The cores were sectioned at a resolution of 1 cm near the surface, increasing to 4 cm for sediment depths greater than 20 cm. For all measurements and sub-sampling for redox-sensitive parameters from the MUC cores, the sediments were sectioned inside an argon-filled glove bag to prevent contact with atmospheric oxygen and filled into 50 ml Falcon tubes. Porewater was extracted by centrifuging the samples at 4000 rpm for 20 minutes at 3°C in a refrigerated centrifuge, effectively separating the porewater from the particulates. Following a mechanical failure of the centrifuge, porewater was obtained by inserting Rhizon filters (0.2 µm) into pre-drilled holes in the lids of the centrifuge tubes. Porewaters were then extracted under vacuum using 20 ml Perspex syringes. All porewater samples were then filtered (0.2 µm cellulose-acetate syringe filters) under argon. Supernatant bottom water samples of the MUC cores were also collected at each station. Additional sediment samples cores were stored at 4ºC in pre-weighed airtight containers for porosity and particulate geochemistry analyses.

For quantification of sulfate reduction rates (SRR), we used the radiotracer incubation technique of Jorgensen (1978). Three acrylic tubes (24 mm internal diameter, 3 mm wall thickness) were carefully inserted into a single MUC core from the same deployment as for the geochemistry analyses using suction to avoid compaction during insertion. The tubes were removed from the sediment, both ends sealed with rubber stoppers and stored in an incubator at approximate in-situ temperature. At the end of each day, $^{35}SO_4^{2-}$ radiotracer solution was injected into the cores, from the water-sediment interface down to 20 cm sediment depth. The radiotracer (15 µl volume, activity ca. 200 kBq) was injected in 1 cm intervals through silicone-sealed holes with 2 mm diameter. The cores were then incubated for 24 h in the dark.

After the incubation, the sediment was pushed out of the acrylic tubes and sectioned. A resolution of 1 cm was selected for the first 6 cm, then 2 cm down to 10 cm, followed by 5 cm for subsequent depths down to 20 cm. Each sediment section was placed in a 50 ml centrifuge tube, pre-loaded with 10 ml of 20% zinc acetate solution to fix all hydrogen sulfide and terminate microbial activity. Samples were thoroughly shaken to break up sediment aggregates and then frozen overnight. Further storage and transport to the home lab was done at room temperature.

2.3 In situ flux measurements with BIGO landers

In situ flux measurements were conducted using two Biogeochemical Observatories (BIGO-I and BIGO-II). The BIGOs were deployed 3 and 7 times in the CL and HI areas, respectively. Each lander had two measurement chambers (C1 and C2) with a diameter of 28.8 cm and an area of 651 cm^2 (Sommer et al., 2009, 2016). Details of lander deployment protocols can be found elsewhere (Sommer et al., 2009, 2016). Sediments were incubated for 30 to 48 hours, and discrete samples (~47 mL) of overlying water were collected at pre-programmed intervals using glass syringes. The glass syringes were connected to the chambers through 1-meter-long Vygon tubes filled with distilled water with a dead volume of 6.9 mL. An additional eight glass syringe water samples were collected to monitor ambient bottom water conditions at the same time intervals. Another sample set was collected for the analysis of DIC and TA in quartz glass tubes. Water samples from the glass syringes were immediately transferred to a cooling laboratory and subsampled for analyses of nitrate (NO_3^-), nitrite (NO_2^-), ammonium (NH_4^+), phosphate (PO_4^{3-}), and silicic acid (H_4SiO_4). Oxygen was measured inside the chambers and in the ambient seawater using optodes (Aanderaa). They were two point calibrated before each lander deployment using well-oxygenated seawater and anoxic seawater, which was produced by adding 5 to 15 g of Na_2S. The dilution error from the distilled water in the glass syringe samples, was corrected using chloride concentrations measured in the syringe samples and the ambient seawater. Nutrient and oxygen fluxes were determined by multiplying slope of the linear regression of the concentration versus time slope by the height of the water inside the chamber. Fluxes determined this way include fluxes by molecular diffusion in addition to non-local transport by bioirrigation and thus constitute the total solute flux. Oxygen fluxes are thus reported as total oxygen uptake (TOU), and as a positive number. Otherwise, reported positive fluxes are directed into the water column and vice versa. Separate BIGO

https://doi.org/10.5194/egusphere-2025-2905
Preprint. Discussion started: 27 June 2025

sediment cores were collected by pushing short liners (10 cm in diameter, approximately 20 cm in length) into the sediment within the incubation chambers after BIGO retrieval. Sediment cores were subsampled, and porewater was extracted similarly to MUC cores. The BIGO incubation chambers were also subsampled for SRR measurements, directly inserting three acrylic tubes into each chamber after recovery of the lander. Samples were treated identical to those from MUC cores.

2.4 In situ flux O_2 measurements with Deep-sea Rover (DSR) Panta Rhei

In addition to the fluxes measured using the BIGOs, the autonomous Deep-Sea Rover (DSR) Panta Rhei was used to repeatedly measure O_2 uptake in the HI and the CL. The DSR represents a six-wheeled vehicle (weight in air 1200 kg, 80 kg in water, dimensions 3 x 2 x 1.7 m (L, W, H)), which is specifically designed to carry out repeated benthic oxygen flux measurements inside two benthic incubation chambers at the front of the vehicle for prolonged time periods of up to one year.

O_2 was measured using fiber-optic O_2 sensors (Pyroscience, Bremen), three were placed inside each flux chamber, two sensors record the O_2 variability in the ambient bottom water. The volume of the two benthic chambers was either determined automatically by injecting pure water into the benthic chambers after the measurement and simultaneously recording the change of the conductivity (Aanderaa conductivity sensors) or by vertical centimeter scales mounted at the outside of each transparent chamber. From these data, the TOU was determined in same way as for the BIGOs. Additionally, the rover carried three camera systems. Two of which are forward looking focusing on the sediment area where flux measurements are conducted by the left and right flux chamber, whereas the third camera is backward looking.

Upon its placement on the seafloor, the following sequence of activities was performed by the rover: i. after placement, it moved a distance of several meters away from its landing site into an undisturbed area, ii. Subsequently, the benthic chambers were flushed, iii. photos taken of the area that will be sampled by the two benthic chambers iv. benthic chambers inserted into the sediment and flushed prior to the start of flux measurement, v. directly thereafter photos taken of both chambers whilst inserted into the sediment (these photos can be used for the volume determination of each chamber), vi. measurement phase, duration was set to 8 hours, the sampling interval of the optodes was set to 5 min. vii. after the measurement phase, pure water was injected to determine the volume of both chambers, and the change of conductivity was monitored for 20 min at an increased sampling rate, viii. the chambers were raised out of the sediment and photos of the sampled area were again taken, ix. the rover advanced 0.7 m to the next measurement area. Apart from step i, this sequence was repeated until the recovery of the rover.

2.5 Geochemical analyses of sediments

Porewater samples were immediately analyzed for TA, dissolved nutrients (TPO_4^{3-}, NO_3^-, NO_2^-, NH_4^+, and H_4SiO_4), Fe^{2+}, and dissolved hydrogen sulfide (H_2S). TA was measured by titrating 0.5–1 mL of sample with 0.02 N HCl using a color indicator (mixture of methylene blue and methyl red), following the method of Ivanenkov and Lyakhin (1978). The endpoint was identified by the appearance of a stable pink color. During titration, the sample was degassed by continuous nitrogen bubbling to eliminate any CO_2 and H_2S produced. Standardization was performed with the International Association for the Physical Sciences of the Oceans (IAPSO) seawater solution, achieving an analytical precision error for TA of better than 3%.

Porewater H_2S, NH_4^+, PO_4^{3-}, and H_4SiO_4 concentrations were determined by standard spectrophotometric methods using a Hitachi U-2001 spectrophotometer (Grasshoff et al., 1999). NO_3^- and NO_2^- were analyzed with a Quaatro Autoanalyzer (Seal Analytic), with an error margin below 2%. Dissolved Fe^{2+} concentrations were measured by taking 1 mL subsamples within a glove bag, stabilizing immediately with ascorbic acid, and analyzing within 30 minutes following complexation with 20 µl of ferrozine. The analytical error for Fe^{2+} measurement was within ±5%. For H_2S analysis, a porewater aliquot was diluted with oxygen-free artificial seawater, and sulfide was fixed by the immediate addition of zinc acetate gelatine solution.

Untreated filtered samples were stored for later SO_4^{2-}, Cl^-, and Br^- analysis via ion chromatography at GEOMAR. Additional subsamples were acidified (20 µl of suprapure HNO_3 added to 2 mL sample) for the analysis of major ions (K, Li, B, Mg, Ca, Sr, Mn, Br, and I) and trace elements by inductively coupled plasma optical emission spectroscopy (ICP-OES). Nutrient concentrations in water samples collected from landers were analyzed using the autoanalyzer, with analytical precision and detection limits reported by Haffert et al., (2013) and Sommer et al. (2025).

https://doi.org/10.5194/egusphere-2025-2905
Preprint. Discussion started: 27 June 2025

The water content of sediment cores was determined at by calculating the difference between the wet and dry weights of the samples. Porosity was then calculated from the water content, assuming a particle density of 2.5 g cm^{-3} and a seawater density of 1.023 g cm^{-3}. After freeze-drying, samples were ground using ball mills. Dry sediment was used for analysis of total carbon, nitrogen (assumed to be particulate organic N, PON) and total sulfur (TS) using a Euro elemental analyzer. POC content was determined after acidifying the sample with HCl (0.25 N) to transform the inorganic carbon to CO_2. Particulate inorganic carbon, assumed to be calcium carbonate ($CaCO_3$), was determined by weight difference between total and organic carbon. The precision and detection limit of the POC analysis was 0.04 and 0.05 dry weight percent (% C), respectively, while that for $CaCO_3$ was 2 and 0.1 % C.

The pyrite content of surface sediments (0 – 1 cm) was estimated by chromium-reducible sulfur following (Canfield et al., 1986). Freeze-dried and ground samples were used. Liberated sulfur was trapped as zinc sulfide and analyzed by photometry (Cline, 1969). The long-term reproducibility and accuracy of the method were monitored against analysis of pure pyrite mixed with quartz sand and an in-house standard (OMZ-2, Peru margin sediment).

Sulfate reduction rates (SRR) were quantified at GFZ Potsdam, using the cold chromium distillation technique (Kallmeyer et al., 2004). The sample vials were centrifuged and the supernatant carefully removed. A small aliquot of supernatant was kept for quantification of total radioactivity and the rest was discarded. The sediment pellet was quantitatively transferred into a distillation flask by flushing it out of the centrifuge vial with a total of 15 mL N, N-dimethylformamide (DMF), technical grade. To ensure complete mixing of the sediment with the chemicals a magnetic stir bar was added to the reaction flask. The flask was then connected to a constant stream of nitrogen gas (approximately 5-10 bubbles per second) in order to maintain strictly anaerobic conditions during the distillation. After 10 minutes of bubbling the DMF-sediment suspension with N_2 gas, 8 mL of 6 M hydrochloric acid (HCl) and 15 mL of 1 M chromium (II) chloride solution were added to the flask via a reagent port. The chemicals will convert all reduced sulfur species (TRIS) to H_2S, which was driven out of solution by the stream of nitrogen gas. The produced gas was then led from the flask through to a first trap filled with 7 mL of a buffered citric acid solution (19.3 g citric acid, 4 g NaOH in 1 L H_2O, pH 4) to trap any aerosols potentially containing unreacted $^{35}SO_4^{2-}$ radiotracer but let all H_2S pass. Finally, the gas was bubbled through 7 mL of 5% (w/v) zinc acetate solution to trap all H_2S as ZnS. To prevent overflowing of the zinc acetate trap, a few drops of silicon-based antifoam were added. After 2 hours of distillation, the contents of the zinc acetate trap, containing the produced $H_2{}^{35}S$ were quantitatively transferred into a 20 mL plastic scintillation vial and mixed with 8 mL scintillation cocktail for quantification of radioactivity by scintillation counting.

Sulfate reduction rates were calculated according to the following formula:

$$SRR = \frac{SO_4 * \varphi * a_{tris} * 1.06 * 10^6}{a_{tot} * t} \quad \text{Eq. (1)}$$

where SRR is the sulfate reduction rate (pmol cm^{-3} d^{-1}); SO_4 is the sulfate concentration in the pore water (mmol L^{-1}); φ is porosity, set to 0.7; a_{tris} is the radioactivity of total reduced inorganic sulfur (cpm); a_{tot} is the total radioactivity used (cpm); t is the incubation time (d); 1.06 is a correction factor for isotopic fractionation; and the factor 10^6 converts from µmol L^{-1} to pmol L^{-1}.

2.6 TA and DIC analysis of water samples

Samples for TA and DIC analysis were taken according to the slightly modified Standard Operation Procedures described by Dickson et al. (2007). The water samples obtained in the glass tubes were transferred into Pyrex test tubes (volume: 10 mL). Subsequently, a small headspace was applied, removing 0.3 mL of the water sample, and the samples were poisoned with 10 µl of $HgCl_2$. The test tubes were closed using greased glass stoppers (Apiezon vacuum grease) secured using plastic clamps, and then stored.

At GEOMAR laboratories, TA (Dickson, 1981) was titrated automatically in an open measuring cell (Metrohm, volume of measuring cell: 1-50 mL) according to Dickson et al. (2007). The sample volume was 1 mL. Hydrochloric acid (0.01 M) was added stepwise and the pH value was continuously recorded using an electrode (Metrohm). The TA concentration was calculated using a modified Gran method (Gran, 1952; Humphreys, 2015). The precision and the deviation from the reference standard were 0.2 and 0.02 %, respectively. The CRM seawater standard Dickson batch #188 was used as the reference standard (total inorganic carbon content: 2099.26 µmol kg^{-1}; total alkalinity: 2264.96 µmol kg^{-1}, https://www.ncei.noaa.gov/access/ocean-carbon-acidification-data-system /oceans/Dickson_CRM/batches.html).

https://doi.org/10.5194/egusphere-2025-2905
Preprint. Discussion started: 27 June 2025

The concentration of DIC was measured according to Dickson et al. (2007) using an Apollo SciTech analyzer (Model AS-C5) equipped with an infrared carbon dioxide (CO_2) detector (Trace Gas Analyzer 7815-01, LICOR). The sample (0.6 mL) was mixed with 0.7 mL H_3PO_4 in an extraction chamber where the DIC is completely converted to CO_2 and measured by infrared spectroscopy. A dilution series of a sodium carbonate standard (Na_2CO_3, 100 mM) was prepared for calibration, whereby salt water (7 g l^{-1} NaCl) was used for the dilution. The CRM standard (batch 188) served as the reference standard. The precision and the deviation from the standard were 0.2 and 0.3 %, respectively.

2.7 Diffusive flux calculations

The diffusive flux of dissolved constituents in porewater between the bottom water and surface sediment was calculated according to Fick's law:

$$J_C = \phi \times D_s \times (dC/dz) \quad \text{Eq. (2)}$$

where J_C represents diffusive flux of solute C at the sediment-water interface, ϕ is porosity, D_s is the diffusion coefficient in sediments, and dC/dz is the concentration gradient at the sediment-water interface. The diffusion coefficient was derived from the diffusion coefficient in seawater (D_{sw}) at in situ temperature and salinity using the following equation (Li and Gregory, 1974):

$$D_s = D_{sw} / \theta^2 \quad \text{Eq. (3)}$$

where θ^2 accounts for sediment tortuosity calculated according to Boudreau (1997):

$$\theta^2 = 1 - \ln(\phi)^2 \quad \text{Eq. (4)}$$

The diffusion coefficient for TA was assumed to be equal to that for bicarbonate ion (Dale et al., 2021a). Concentrations of TA, NH_4^+, and H_4SiO_4 gradually increased with sediment depth, which allowed the concentration gradient to be calculated by taking the derivative at the sediment-water interface of an exponential function fitted through the concentration data in the upper 4 cm:

$$C(z) = \alpha - (\alpha - C(0)) \times e^{-\gamma z} \quad \text{Eq. (5)}$$

C(z) – concentration at depth z
α – asymptotic concentration at 4 cm depth
C(0) – bottom water concentration
γ – exponential coefficient
z – sediment depth

The best fit to the data was determined using the FindFit function in Mathematica software. Concentrations of Fe^{2+}, NO_3^-, NO_2^-, H_2S and PO_4^{3-} were more scattered and did not easily lend themselves to Eq. (5), and their diffusive fluxes were not calculated.

2.8 POC degradation rate calculations

The rates of particulate organic carbon degradation ($RPOC_{TOT}$) were estimated using a mass balance approach based on the measured fluxes (F) of O_2, NO_3^-, and NH_4^+ (Dale et al., 2014):

https://doi.org/10.5194/egusphere-2025-2905
Preprint. Discussion started: 27 June 2025

$$RPOC_{TOT} = \frac{r_{CN}(2\,F_{NH4}\,r_{NO3} - F_{O2}\,r_{NO3} - F_{NH4}r_{O2} - F_{NO3}\,r_{O2})}{2\,r_{NO3} - r_{O2} + r_{CN}\,r_{NO3}\,r_{O2}} \quad \text{Eq. (6)}$$

where r_{CN} represents the atomic ratio of carbon-to-nitrogen (C:N) ratio in organic matter undergoing degradation, calculated from the mean down-core POC and PON contents. r_{O2} and r_{NO3} were stoichiometric ratios of 118/106 and 94.4/106, respectively, assuming organic matter with an oxidation state of -0.45 (Dale et al., 2014).

2.9 Statistical analyses

Statistical analyses were conducted using the R software package. The non-parametric Mann-Whitney U test was employed for each set of data to assess the variability of fluxes between the HI and CL areas. Additionally, this test was also utilized to understand the difference in porewater profiles and variability in the particulate data between HI and CL areas. A *p*-value <0.05 was considered indicative of statistically significant variability.

3. Results

3.1 Environmental conditions at Mecklenburger Bight

Environmental conditions were monitored during the experiment from 18 July to 9 August 2024 using shipboard measurements of wind speed, wind direction, and surface water temperature (Fig. 2). Additionally, bottom water temperature and dissolved oxygen levels were measured during the different deployments of the DSR. Wind speed varied between 4.4 and 13.7 m s^{-1}, with the highest gusts from a northwesterly direction. Correspondingly, sea surface temperature (SST) generally ranged between 18 and 20 °C with an increase to 21 °C by 1 August. The bottom water temperature, initially recorded at 9.8 °C, rose to 10.6 °C over the study period. Between 18 July and 2 August, bottom water O_2 levels declined from approximately 100 µmol L^{-1} to a minimum of 46 µmol L^{-1}. Notable fluctuations in O_2 concentrations were recorded between 31 July and 2 August, which coincided with reduced wind speeds and northerly winds. These variations were likely influenced by wind speed oscillations between 0.5 and 6 m s^{-1}, inducing seiches along the sloping seabed, where water masses of different O_2 concentrations flowed past the rover.

A cyanobacterial bloom appeared in the study area between 3 and 6 August. During this period, SST ranged from 20.1 to 21.4 °C. In contrast, bottom water temperature remained decoupled from diurnal surface temperature fluctuations, gradually increasing from 9.7 to 10.3 °C. Simultaneously, bottom water O_2 concentrations increased from 34 to 94 µmol L^{-1}. The variations in bottom water temperature and O_2 levels may be influenced by wind forcing, particularly a shift in wind direction from strong alongshore westerly winds to moderate southeasterly winds.

https://doi.org/10.5194/egusphere-2025-2905
Preprint. Discussion started: 27 June 2025

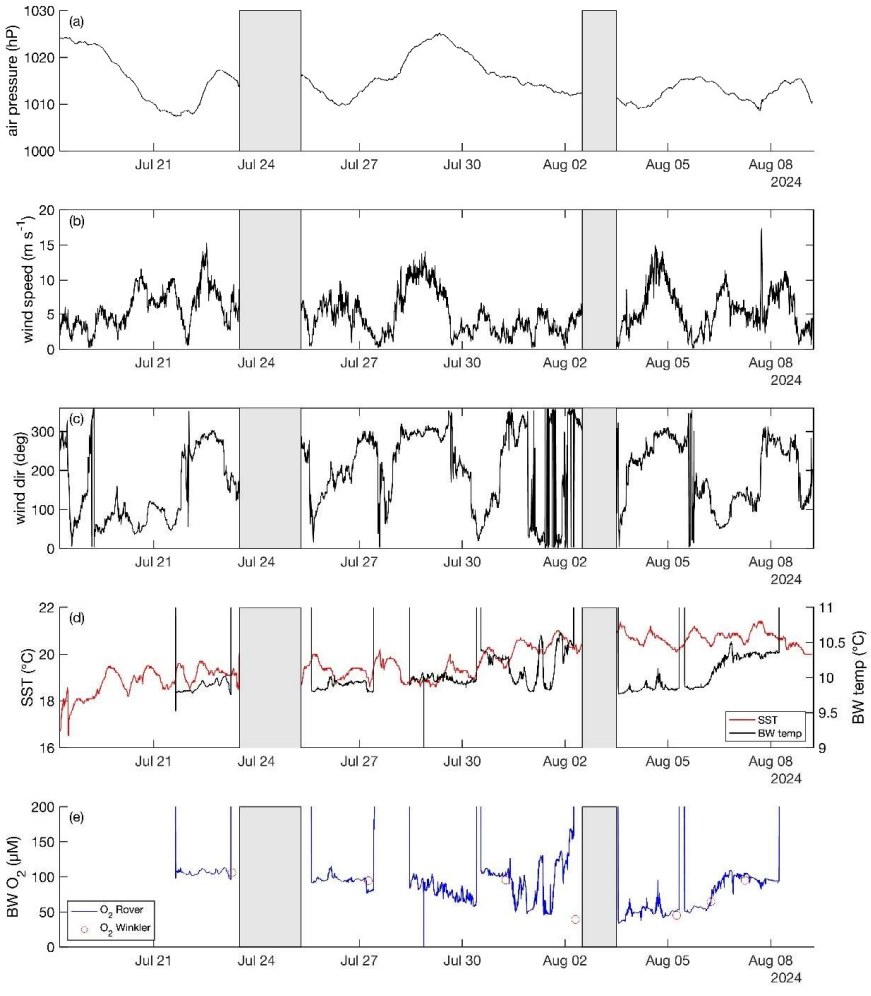

Figure 2: Environmental conditions during the time course of the trawling experiment including (a) air pressure, (b) wind speed, (c) wind direction, (d) SST (red) and bottom water temperature (black), (e) bottom water dissolved O_2 concentration. Grey bars indicate periods where the ship returned to harbor.

Initially, the thermocline and halocline were located at around 10 m depth and later shifted downwards due to the increase in wind velocity and mixing of the surface layer (Fig. 3). This shift was accompanied by a corresponding deepening of the nutricline. Over time, the chlorophyll-a maxima intensified to almost 15 µg L^{-1} when the cyanobacterial bloom intensified. In the surface mixed layer, O_2 concentrations were around 300 µmol L^{-1} and declined to ~110 µmol L^{-1} at 4 m above the seafloor. Note that the low O_2 concentrations <100 µmol L^{-1} recorded by the DSR (Fig. 2) at a distance of ~70 cm above the sediment were not detected by the CTD (maximum depth 5 m above the seafloor).

https://doi.org/10.5194/egusphere-2025-2905
Preprint. Discussion started: 27 June 2025

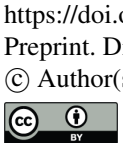

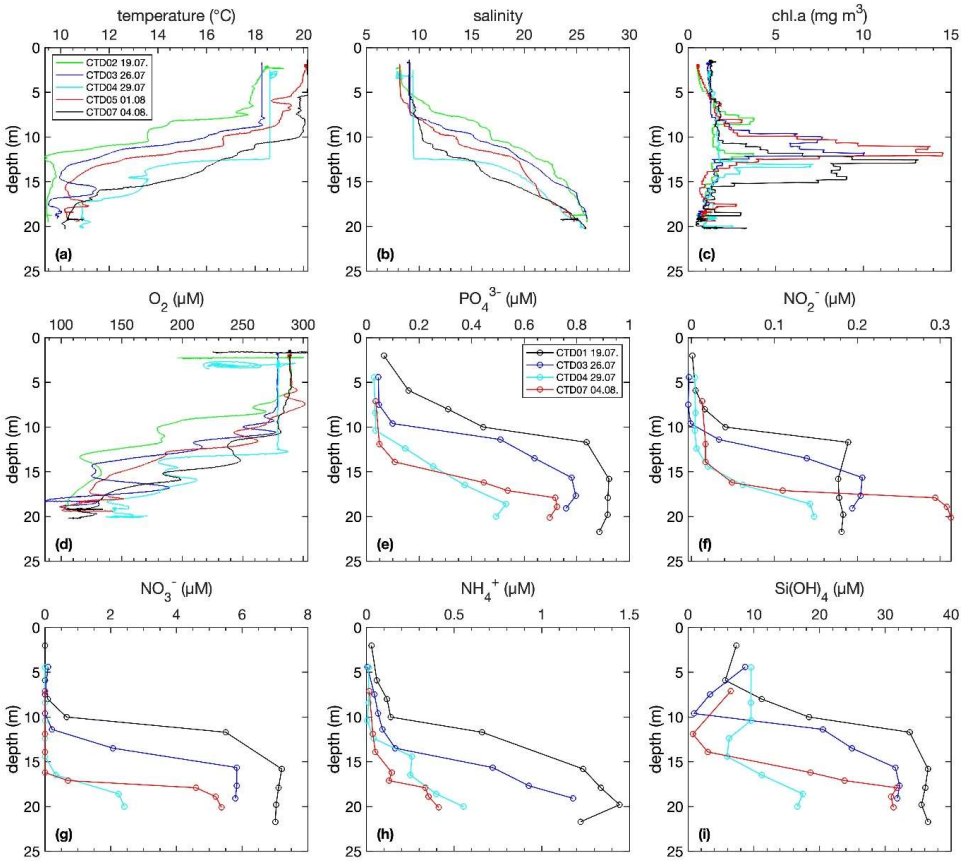

Figure 3: Water column distributions of profiles of temperature, salinity, chlorophyll-a, nutrients and oxygen. Note that technical issues were observed with the pumps of CTD03 and CTD04, affecting temperature, salinity, and O_2 in the upper 12 m.

3.2 Trawling disturbance

The disturbance caused by the otter boards and footrope on the seafloor morphology is distinctly visible in Fig. 4. The images show the undisturbed seabed on the left, characterized by a thin layer of brown phytodetritus. Moving to the right, a sharply defined furrow created by the left trawl board exposed the underlying dark-grey anoxic sediment. A narrow strip of relatively undisturbed sediment is observable adjacent to the furrow, followed by sediment piles cast inwards by the otter boards. Further to the right of the sediment casts, another narrow zone of minimally disturbed sediment can be observed. Finally, at the far right of the image, the sediment surface in the net zone has been visibly scraped by the footrope and rollers dragging across the seafloor during bottom fishing. A large sediment plume was also observed on the camera system immediately after trawling (not shown).

https://doi.org/10.5194/egusphere-2025-2905
Preprint. Discussion started: 27 June 2025

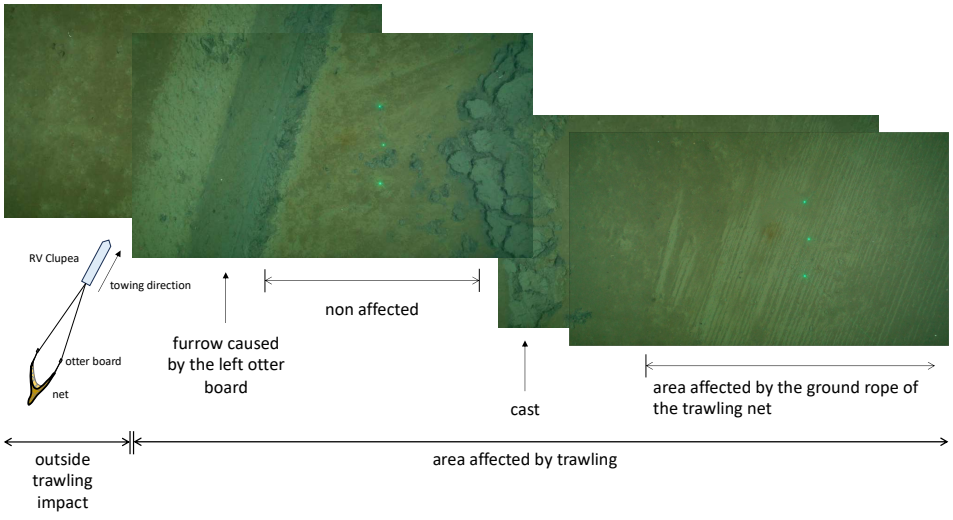

Figure 4: Ocean Floor Observation System (XOFOS) images taken across a trawl mark caused by the left otter board and the net area affected by the footrope. The distance between the outer two green laser points is 45 cm. During trawling, the trawl door penetrates the sediment surface, displacing material from the furrow and depositing it towards the inner side. The area affected by the footrope was targeted for sampling in the HI area. Details of the XOFOS deployments are provided in Sommer et al. (2025)

3.3 Sediment biogeochemistry and fluxes

Mean contents of POC, PON, $CaCO_3$ and TS are presented in Fig. 5 and Table S2, along with organic C:N ratios. The sediment can be classified as organic-rich and carbonate-poor. POC, PON and $CaCO_3$ all decreased markedly in the upper 10 cm, and then stabilized at greater depth. TS, in contrast, accumulated to ~ 1 wt. % S. C:N ratios increased from ~ 8 to 9, indicating preferential remineralization of PON relative to POC. All particulate species in the HI area exhibited a slight reduction in the top 2-3 cm compared to the CL area. The reduction of POC in the HI area was close to 1 wt.%. These differences are statistically significant in the upper 1.5 cm. Taken at face value, the data suggest that sediment removal by the footrope amounted to the upper 1-2 cm.

Surface pyrite contents in the CL area (0.47 ± 0.07 wt.% FeS_2) were somewhat higher than the HI area (0.41 ± 0.14 wt.% FeS_2) although the differences were not statistically significant.

https://doi.org/10.5194/egusphere-2025-2905
Preprint. Discussion started: 27 June 2025

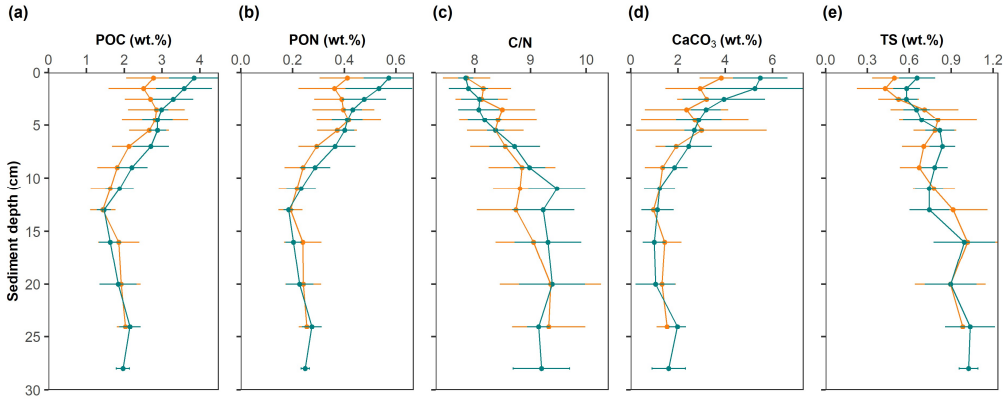

Figure 5: Solid-phase profiles at the study site. Mean values and standard deviations are shown for control sites (green) and high-impact areas (orange).

Mean solute concentrations measured in MUC samples from CL and HI sites exhibited similar trends (Table S3, Fig. 6). The data have been normalized to chloride concentrations to account for down-core changes in salinity (Fig. 6i). Concentrations of TA, NH_4^+, PO_4^{3-} and H_4SiO_4 increased with depth due to the remineralization of organic matter. Concurrently, SO_4^{2-} decreased by ~4 mM in the upper 10 cm and then showed little further decrease with depth. Concentrations of H_2S were low in the upper 5 cm where a pronounced Fe^{2+} peak was observed. H_2S then increased to ~200 µM at the bottom of the cores. NO_3^- concentrations were elevated in the top 2 cm and then remained at levels close to the detection limit further down.

SR rates in these organic-rich sediments were elevated very close to the sediment surface and then decreased quasi-exponentially down to ~15 cm. The depth-integrated SRR equaled 3.9 and 4.9 mmol S m^{-2} d^{-1} at the CL and HI sites, respectively. For a simple carbohydrate (i.e. zero C oxidation state), 2 moles of POC are oxidized per mole of SO_4^{2-} reduced (e.g., Burdige and Komada, 2011). The SRR thus translates to a POC oxidation rate of roughly 8 and 9 mmol m^{-2} d^{-1} at the CL and HI sites.

Concentrations of TA, NH_4^+, PO_4^{3-}, H_4SiO_4 and Fe^{2+} tended to be higher in the upper cm in the CL area compared to the HI area. Conversely, SO_4^{2-} tended to be lower, whereas H_2S showed little difference. Analysis of the data indicates significant differences between the CL and HI areas for TA within the 1.5 – 5.5 cm depth range and for NH_4^+ within the 0.5 – 9.0 cm depth range. For the remaining variables, there were no statistically significant differences.

https://doi.org/10.5194/egusphere-2025-2905
Preprint. Discussion started: 27 June 2025

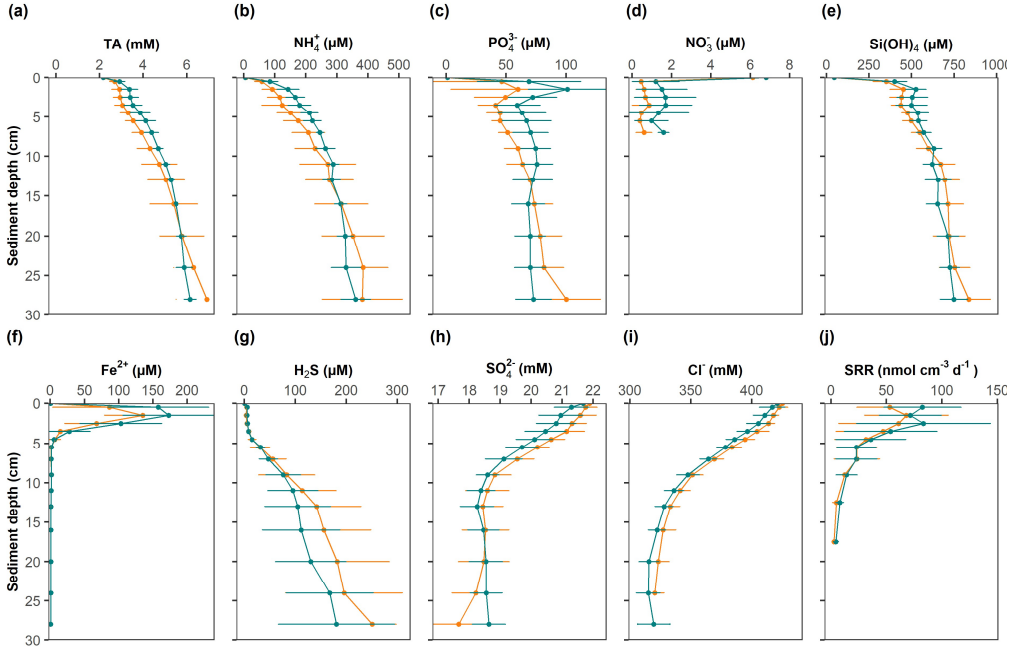

Figure 6: Solute concentrations in porewaters at the study site and SR rates. Mean concentrations and standard deviations are shown for control sites (green) and high-impact areas (orange).

Total fluxes (BIGO data) and diffusive fluxes (for TA, NH_4^+, and H_4SiO_4) are illustrated in Fig. 7 (and Table S3). For TA and NH_4^+, the two approaches were consistent with regards to the range and magnitude of the fluxes. H_4SiO_4 fluxes showed larger differences with lower fluxes associated with the BIGO data. In general, the sediments were a sink for O_2 and NO_3^- and a source for all other variables. NO_2^- effluxes (not shown) were < 0.05 mmol m^{-2} d^{-1}. Mean TOU in the control area was 8.9 mmol m^{-2} d^{-1}, whereas DIC fluxes were much higher (mean19.5 mmol m^{-2} d^{-1}), implying a significant contribution of carbonate dissolution to the DIC flux. This is also supported by a very high mean TA flux of 12.2 mmol m^{-2} d^{-1} in the CL area. Following trawling, the fluxes of TOU, TA, DIC, NH_4^+, PO_4^{3-}, H_4SiO_4 all declined compared to the CL area, whereas NO_3^- and NO_2^- fluxes showed little change. Notably, mean TA and DIC fluxes were much lower in the HI area, falling to 5.4 and 10.2 mmol m^{-2} d^{-1}, respectively. The lower fluxes of TA, NH_4^+, PO_4^{3-} and H_4SiO_4 following trawling are further consistent with the lower porewater concentrations. The net fixed N flux ($\sum NH_4^+ + NO_3^- + NO_2^-$) was always directed to the water column, but was reduced by trawling (not shown). Fluxes of TA, DIC, O_2, NH_4^+, PO_4^{3-}, and H_4SiO_4 exhibited statistically significant differences between the HI and CL areas.

Control area estimates of $RPOC_{TOT}$ equaled 8.7 mmol m^{-2} d^{-1}, and were followed by a statistically significant decrease after trawling to 7.1 mmol m^{-2} d^{-1} (Fig. 7h). These are very similar to the TOU, which provides confidence in the $RPOC_{TOT}$ calculation. They are also similar to the depth-integrated SRR calculated above. Sulfate reduction is thus the major carbon remineralization pathway, as expected for organic-rich coastal sediments (e.g. Jørgensen, 2021; van de Velde et al., 2018).

Over the 16-day observation period in the HI area, the BIGO fluxes exhibited temporal variability, likely reflecting the gradual recovery of environmental conditions post-trawling (Fig. 8). TA and DIC effluxes and TOU apparently did not fully recover to the CL values by the end of the sampling program. Temporal trends in the fluxes of NH_4^+, PO_4^{3-}, and H_4SiO_4 were less clear, although there is a tendency for higher fluxes in the CL area versus the HI area.

https://doi.org/10.5194/egusphere-2025-2905
Preprint. Discussion started: 27 June 2025

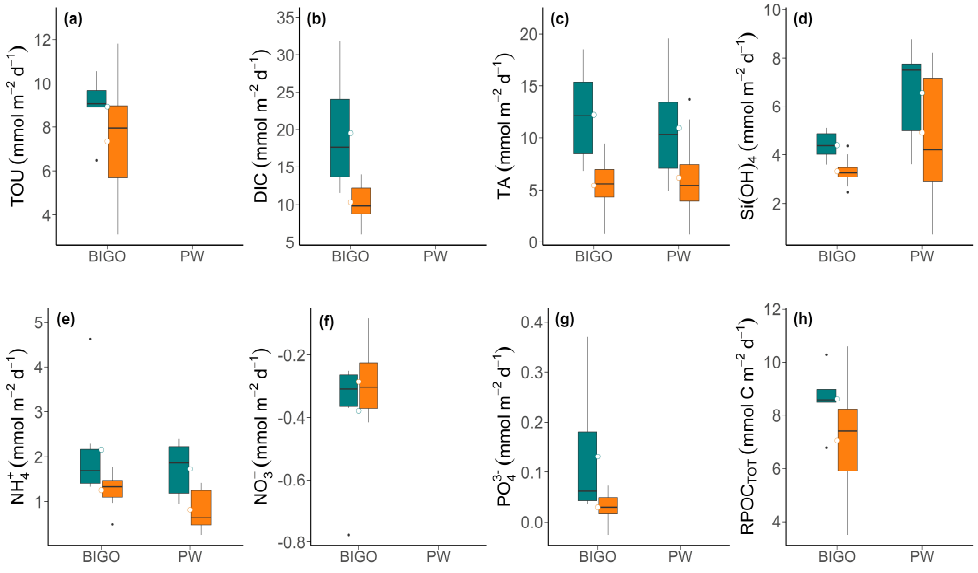

Figure 7: (a-g) Box-whisker plots showing the fluxes of solutes fluxes across the sediment-water interface calculated from lander data (BIGO) and porewater profiles (PW) at the control (green) and high-impact sites (orange). Mean fluxes are shown by the small circles. (h) POC remineralization rates were calculated using Eq. 5.

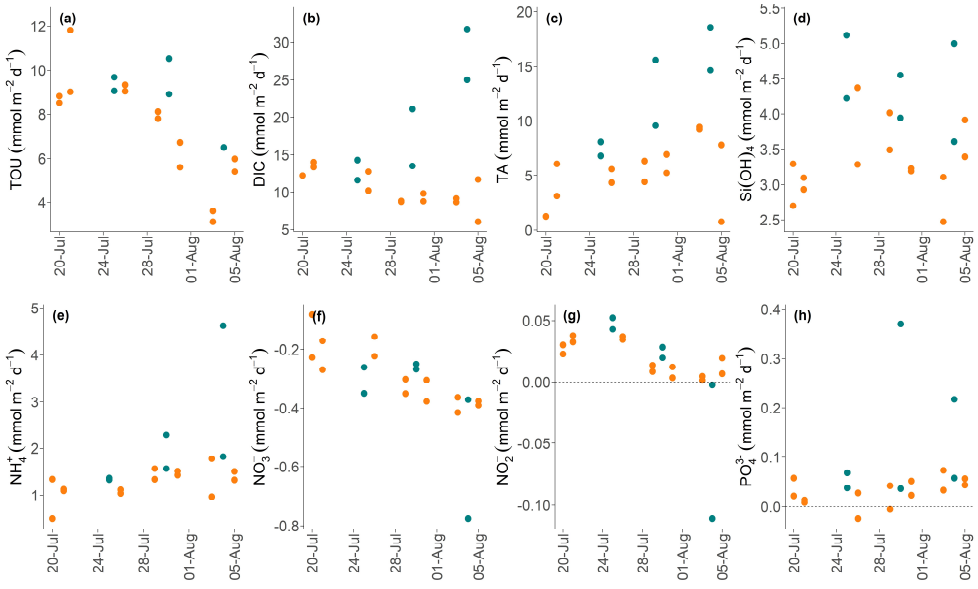

Figure 8: Plots showing the temporal evolution of total fluxes of solutes across the sediment-water interface (in mmol m^{-2} d^{-1}) over 16 days in control (green) and high-impact (orange) areas determined from the BIGO data. Dashed horizontal lines indicate zero flux.

https://doi.org/10.5194/egusphere-2025-2905
Preprint. Discussion started: 27 June 2025

4. Discussion

4.1 Changes in TOU and nutrient fluxes in the net zone

The seafloor photographic images strikingly demonstrate the impact of trawling on sediment morphology (Fig. 4). Sediment was unevenly tossed into the net area by the otter boards, as evident in previous benthic images and model simulations (Bradshaw et al., 2021; Ivanović et al., 2011). In this study, we provide a comprehensive data set on biogeochemical fluxes based on in situ measurements using benthic landers, including DIC and TA fluxes. Focus is on the 60 m wide net zone where the net footrope scrapes across the seafloor. The net area is far larger than that disturbed by the otter boards (1 – 2 m). Besides, for practical reasons, it was not possible to target the narrow mound and furrows gauged out by the otter boards with our large lander and coring equipment. The trawl marks were sampled by SCUBA divers using push cores, and this data set will be published in a forthcoming manuscript.

An important finding of the study relates to the fluxes measured using BIGO data and porewater gradients. The two approaches exhibited slight differences in magnitude for TA and NH_4^+, whereas BIGO H_4SiO_4 fluxes were notably lower (Fig. 7). This mismatch could be of some concern since biogenic silica recycling efficiencies are often calculated using porewater concentration gradients (Dale et al., 2021b). Porewater fluxes derived from concentrations measured in 1-cm intervals fail to capture the porewater gradients just below the sediment surface and do not account for non-diffusive fluxes arising from bioirrigation (Apell et al., 2018). In contrast, the fluxes obtained from benthic chambers integrate all the net sources and sinks across the sediment surface (Tengberg et al., 1995). Since porewater concentrations of H_4SiO_4 were higher than in the bottom water, bioirrigation would tend to flush out H_4SiO_4 and augment the total flux. A large sink for H_4SiO_4 in the upper centimeter could account for the lower BIGO fluxes, although we find this hard to envisage given current knowledge about silica cycling in marine sediments (DeMaster, 2003). The lower benthic chamber fluxes thus suggest that the curve fitting procedure overestimates the H_4SiO_4 flux at Mecklenburger Bight, but not for TA and NH_4^+.

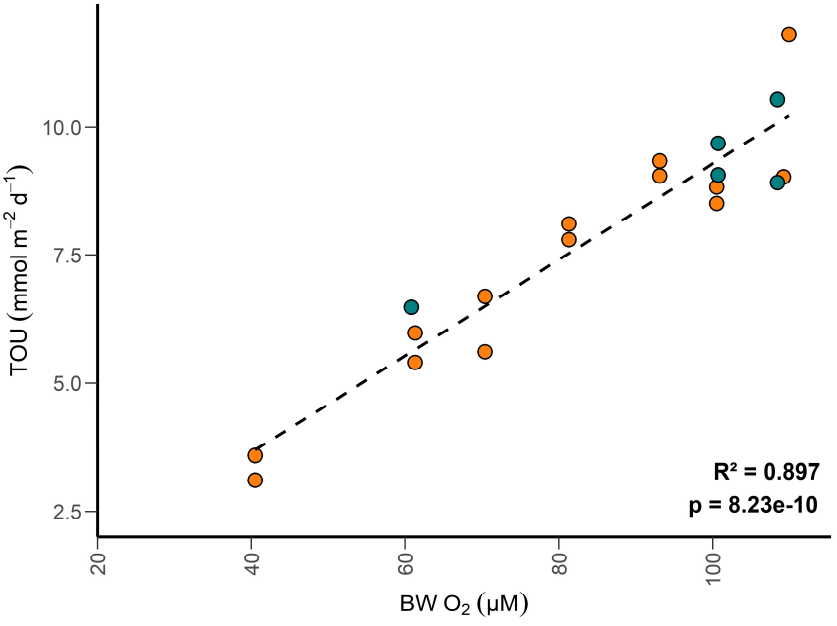

Figure 9: TOU versus bottom water oxygen concentration measured by the rover in control (green) and high-impact (orange) areas.

https://doi.org/10.5194/egusphere-2025-2905
Preprint. Discussion started: 27 June 2025

Oxygen concentrations in surface sediments are primarily regulated by the metabolic activities of micro-, meio-, and macrofauna, as well as the oxidation of reduced substances such as NH_4^+, Fe^{2+} and H_2S (Glud, 2008). TOU is further regulated by the content of reactive POC and the bottom water O_2 concentrations. At concentrations < 125 µM, characteristic of our study site, TOU is predicted to correlate positively with bottom water O_2 concentrations (Cai and Reimers, 1995). Above 125 µM, the amount of organic carbon in the sediment becomes the critical factor. Our data show this behavior clearly (Fig. 9). The decline in bottom water O_2 concentrations over the study period (Fig. 2) proves to be an important control on TOU. Previous research has reported that trawling lowers O_2 consumption rates in sedimentary ecosystems by effectively stripping away surface sediments and associated microbial and faunal communities and by diminishing the availability of labile reduced substances (Allen and Clarke, 2007; Tiano et al., 2019; Bradshaw et al., 2024). Our findings suggest, perhaps surprisingly, that trawling has a relatively minor impact on TOU flux in the HI area compared to the role of bottom water depletion. We ascribe this to transport limitation of O_2 across the diffusive boundary layer when O_2 levels begin to fall over time (Bouldin, 1968; Middelburg and Levin, 2009).

The reduction in benthic NH_4^+ fluxes post-trawling contrasts with Morys et al. (2021), who reported an increase immediately afterwards. They attributed this to NH_4^+-enriched porewater at the newly formed sediment-water interface and the subsequent diffusion of NH_4^+ to the bottom water. Similarly, Duplisea et al. (2001) reported that the NH_4^+ flux from trawled sediment was 45 times higher than the flux from undisturbed sediments. Our findings align more with Bradshaw et al. (2021), who observed a decrease in NH_4^+ flux and argued that it was caused by NH_4^+ depletion following surface sediment removal or from a deceleration of biogeochemical turnover rates. Almroth-Rosell et al. (2012) also found that sediment resuspension resulted in decreased NH_4^+ efflux (~50%) in a benthic chamber investigation, which they ascribed to oxidation of NH_4^+ stimulated by nitrification (Almroth-Rosell et al., 2012). We argue for a simpler explanation, whereby the lower NH_4^+ fluxes are caused by removal of the reactive surface layer associated with the highest rates of ammonification; a finding unambiguously borne out by the reduction in DIC and TA fluxes, as well as by diagenetic modelling (De Borger et al., 2021). The same reasoning applies to the reduction in H_4SiO_4 fluxes. The dissolution of biogenic silica, mainly diatoms in the Baltic Sea, is the main source of silicate in porewaters (Tréguer and De La Rocha, 2013). Given that dissolution rates are highest at the sediment surface where opal undersaturation is greatest (Rabouille et al., 1997), it logically follows that removal of this layer will immediately diminish the benthic H_4SiO_4 flux.

Mean fluxes of NO_3^- into the sediment (0.3 – 0.4 mmol m^{-2} d^{-1}) were not significantly different between the CL and HI sites, suggesting that denitrification rates in the net area remained stable despite trawling activities. Model results by De Borger et al. (2021) applicable to the net area predicted that increased oxygenation due to bottom trawling may double denitrification rates by enhancing NO_3^- availability, possibly due to higher rates of coupled nitrification-denitrification. In contrast, intensive fishing activities may reduce NO_3^- concentrations through increased microbial activity, excessive sediment mobilization, and net N loss from sediments (Hale et al., 2017). Ferguson et al., (2020) also reported that benthic trawling altered sediment redox profiles and reduced denitrification rates by 50%. This variability of the trawling impact on the direction of the benthic fixed N source/sink highlights the confounding complications of site-specific environmental factors, such as benthic fauna, nutrient availability and oxygen penetration depth (Sciberras et al., 2016).

Our data nonetheless show that trawling leads to a net decline in the benthic fixed N source to the water column. The exact fate of the N loss (i.e. increased denitrification versus porewater NH_4^+ efflux to the water column) is difficult to constrain and would require detailed laboratory studies to gain further insight. However, combined with the lower PO_4^{3-} flux (as also observed by Bradshaw et al., 2021), trawling might have broader consequences for the productivity of the water column. A modeling study reported that trawling reduces biomass production by 56 % in the North Sea (Hiddink et al., 2006). Post-trawling porewater concentrations of PO_4^{3-} were elevated immediately below the sediment surface (Fig. 6), and it follows that scraping by the footrope trawling mixes surface porewater PO_4^{3-} into the lower column, as previous findings have shown (Bradshaw et al., 2021; Duplisea et al., 2001; Sciberras et al., 2016). We currently lack data on bottom water chemistry immediately after trawling, to track the missing PO_4^{3-} after sediment resuspension. Since P cycling in sediments is to a large degree controlled by the redox cycling of Fe (Slomp et al., 1996), it remains to be shown whether the lower PO_4^{3-} flux was instead caused by adsorption onto freshly formed iron oxide following resuspension (Almroth-Rosell et al., 2012). The observed reduction in porewater Fe^{2+} concentrations after trawling could be evidence for this, although presently this is only speculation.

https://doi.org/10.5194/egusphere-2025-2905
Preprint. Discussion started: 27 June 2025

Despite the large number of in situ lander operations over the 16-day experimental period, the recovery time of the sediments with regards to fluxes is difficult to unequivocally reconcile for all chemical components (Fig. 8). DIC, TA and H_4SiO_4 were consistently higher in the undisturbed control area, whereas for the other nutrients the HI fluxes seemed to converge to the CL fluxes soon after trawling. Yet, the temporal variability of the control fluxes makes it hard to define a robust control baseline, and this is a crucial point that should be noted for all published and planned fieldwork studies on this topic. The temporal decrease in bottom water O_2 is an additional complication since will affect the rates of carbon cycling and associated redox processes. However, results from long-term (~weeks) ex situ core incubations in the oxygen minimum zone off NW Africa show that benthic fluxes only begin to be altered when dissolved O_2 falls below ~20 µM and with a time lag of 1-2 days (Schroller-Lomnitz et al., 2019). Bottom water dissolved O_2 at Mecklenburger Bight was consistently above this threshold (Fig. 2).

4.2 Bottom trawling and organic carbon remineralization

The organic carbon remineralization rate calculated from our benthic flux measurements ($RPOC_{TOT}$) showed a decline following trawling activities. This reduction is further evident from the in situ DIC and TOU flux measurements. Understanding the impact of trawling on ocean carbon storage is key to predict anthropogenically-induced changes to the benthic carbon cycle, yet remains a subject of considerable debate (Epstein et al., 2022; Zhang et al., 2024). Trawling-induced mechanical disturbance can increase the oxygen exposure of POC buried in sediments, thereby promoting aerobic remineralization and subsequently affecting atmospheric CO_2 uptake (Atwood et al., 2024; Sala et al., 2021). Although oxygen exposure is a major control on organic matter remineralization (Dauwe et al., 2001), other factors are also important. These include composition of associated biological communities such as microbes, particle grain size and mineralogy as well as, the local hydrodynamic conditions (Aller et al., 1996; Arnosti and Holmer, 2003; Burdige, 2007; Hedges and Keil, 1995).

The surface layer of the sediments holds a high abundance of microbial and macrofaunal communities (Dauwe and Middelburg, 1998; Watling et al., 2001). Our data imply that the upper 2 cm might have been scraped away by the ground rope, in agreement with other trawling experiments (Tiano et al., 2019; Bradshaw et al., 2021). The physical disturbance of the surface sediments along with the removal of fauna may decelerate biogeochemical processing and thereby reduce carbon remineralization rates (De Borger et al., 2021; Morys et al., 2021; Pusceddu et al., 2014; Tiano et al., 2019). Fishing experiments conducted in the North Sea reported a decline in benthic metabolic activity immediately after sediment disturbance (Tiano et al., 2019), whereas other model studies suggest little change (Rooze et al., 2024) or even an increase (e.g. van de Velde et al., 2018).

Sediment grain size plays a crucial role in POC remineralization, since fine-grained particles act as preservation nuclei for organic carbon (Hedges and Keil, 1995). A sediment resuspension experiment conducted in the Kiel Bight (Baltic Sea) suggests that grain size controls the difference between remineralization rates under oxic and anoxic settings (Kalapurakkal et al., 2025). At Mecklenburger Bight, the sediments are predominantly fine-grained, which should help to protect against carbon remineralization by adsorption onto mineral surfaces. However, although the abundance of fine-grained sediment plume was very prominent, we made no attempt to determine the fate of sediment resuspended in the sediments. Furthermore, Tiano et al. (2019) observed that while reductions in total organic carbon may be subtle, bottom trawling disproportionately affects the more reactive fractions of organic carbon. In certain depositional environments, fine-grained suspended sediments may be transported and redeposited in different locations, potentially increasing seabed POC content in downstream areas (Epstein et al., 2022; Palanques et al., 2014). Continuous scraping and ploughing of the surface sediments can also lead to the enrichment of POC due to the upliftment of organic-rich deeper sediments (Palanques et al., 2014). Based on the evidence at hand, we suggest that the categorical reduction in POC remineralization rates shown by our flux measurements can be attributed to the curtailment of biological respiration caused by the removal of the sediment surface.

4.3 Impact of benthic alkalinity losses on air-sea CO_2 fluxes

Literature discussions on the impact of trawling on air-sea CO_2 exchange have focused on the oxidation of resuspended organic carbon as the principle agent of enhanced CO_2 release (Atwood et al., 2024; Hiddink et al., 2023; Sala et al., 2021). Yet, it has recently been shown that pyrite oxidation in the water column induced by sediment resuspension has a far higher potential to induce CO_2 emissions to the atmosphere and a weakening of

https://doi.org/10.5194/egusphere-2025-2905
Preprint. Discussion started: 27 June 2025

the carbon shelf pump (Kalapurakkal et al., 2025). Our results add to this body of knowledge by showing that trawling also causes a large and immediate reduction in benthic DIC and TA emissions by roughly 50 % (by 9.2 and 6.7 mol m^{-2} d^{-1}, respectively), which then persists for at least two weeks. At present, a biogeochemical explanation for this decrease is not possible with the available data. From a benthic perspective, our data demonstrate a dramatic alteration of ecosystem functioning and structure. To the best of our knowledge, our data are the first in situ measurements of TA and DIC fluxes in the net area disturbed by trawling.

Data on TA fluxes determined in situ using benthic chambers in the Baltic Sea are rare in general. Previously, we have measured with our BIGO landers TA fluxes of 7 – 23 mmol m^{-2} d^{-1} in the Fehmarn Belt (east of Bornholm Island) and fluxes of 8 – 30 mmol m^{-2} d^{-1} in fine-grained sediments of the Eastern Gotland Basin (unpublished data). High benthic TA release thus appears to be characteristic of muddy sediments in the Baltic Sea, which may in large part be caused by benthic carbonate dissolution (Wallmann et al., 2022). In muddy Baltic Sea sediments, carbonate dissolution is driven by mineral undersaturation in a thin subsurface layer arising from the acidity produced by aerobic respiration pathways (Dale et al., 2024). Carbonate dissolution results in the release of two moles of alkalinity per mole of DIC:

$$CaCO_3 + CO_2 + H_2O \rightarrow 2HCO_3^- + Ca^{2+} \quad \text{Eq. (7)}$$

An estimate of carbonate dissolution rates (R_{CaDiss}, mmol $CaCO_3$ m^{-2} d^{-1}) in the CL area can therefore be made as follows (e.g. Burdige, 2006; Hammond et al., 1996):

$$R_{CaDiss} = 0.5 \cdot (J_{TA} + J_{NO3} - J_{NH4} - 4 \times J_{PyB}) \quad \text{Eq. (8)}$$

where J_{TA} (12.2 mmol m^{-2} d^{-1}) is the mean TA flux at the CL sites, J_{NO3} is the NO_3^- influx into the sediment (0.38 mmol m^{-2} d^{-1}) and J_{NH4} is the ammonium efflux (2.2 mmol m^{-2} d^{-1}). The burial flux of pyrite J_{PyB} (as moles of FeS_2) has been calculated to be 0.16 mmol m^{-2} d^{-1} using the model described below. The burial flux is multiplied by 4 since each mole of buried S equates to the release of 2 moles of TA. Inserting the numbers gives R_{CaDiss} = 4.5 mmol m^{-2} d^{-1}, or 9 mmol TA m^{-2} d^{-1}, which demonstrates that carbonate dissolution is a likely candidate for the bulk of the measured TA flux.

Given widespread trawling activities in the region, it is pertinent to question the broader impact of a ramping down of benthic TA and DIC source by bottom fishing on CO_2 exchange with the atmosphere. A coupled benthic-water column model was used to estimate the impact. The model was previously used to examine the impact of sediment resuspension on air-sea CO_2 exchange in the western Baltic Sea (Kalapurakkal et al., 2025). The sediment compartment accounts for the rain rate of POC to the seafloor, degradation of POC coupled to pyrite production, pyrite oxidation caused by shallow trawling (upper 2 cm, i.e., resuspension by net scraping) and pyrite and POC burial. Also considered is the enhanced degradation of POC by exposure to oxygen following trawling although, as mentioned, this has only a minor impact on CO_2 fluxes compared to that induced by pyrite oxidation. The corresponding benthic DIC and TA fluxes are fed directly back to the well-mixed water column compartment in a fully coupled manner. In the water column, there is lateral exchange of TA and DIC, and a flux of CO_2 to or from the atmosphere depending on the strength of the benthic TA and DIC emissions.

Initial environmental parameters were set to the study site values (water depth, salinity, temperature, water column DIC and TA concentrations). The molar ratio between pyrite formation and POC oxidation was adjusted to match the local pyrite contents in CL sediment (0.47 wt.%). Following Kalapurakkal et al. (2025), trawling was assumed to disturb 50 % of the seabed, with one trawling event per year that oxidizes the upper 2 cm over a five-day period. Benthic DIC fluxes in the original model were exclusively driven by POC degradation, whereas TA fluxes are driven by pyrite burial and oxidation. In this study, the model was modified in two ways; (i) to include constant values of carbonate dissolution at the derived rates of 9 mmol TA m^{-2} d^{-1} and 4.5 mmol DIC m^{-2} d^{-1}, and (ii) during each trawling event, the benthic DIC and TA fluxes were reduced by 9.2 and 6.7 mol m^{-2} d^{-1} in accordance with the data, and for a period of 21 days. A description of the empirical constraints on trawling frequencies and depths can be found in Kalapurakkal et al. (2025). Our updates to the model are described in the Supplement.

https://doi.org/10.5194/egusphere-2025-2905
Preprint. Discussion started: 27 June 2025

The model results show that each trawling episode leads to pronounced losses of TA, as expected from previous results (Kalapurakkal et al., 2025). Sediments transition from a TA source to a large TA sink during the first trawl due to pyrite oxidation ("Standard run" red curve in Fig. 10a). TA fluxes decrease for each subsequent trawling event due to a long-term impoverishment of pyrite stocks (Kalapurakkal et al., 2025). The water column is a continuous source of CO_2 to the atmosphere at the study site, with large emission peaks consistent with the pulse of acidity produced by oxidation of resuspended pyrite ("Standard run" red curve in Fig. 10b).

In a second execution of the model, DIC and TA fluxes were not reduced by 9.2 and 6.7 mol m^{-2} d^{-1} during trawling. A comparison of the results of this exercise ("No impact" black curves in Fig. 10) with the standard run shows that the observed reduction in TA and DIC fluxes by trawling has a very minor, almost negligible, impact on TA fluxes and CO_2 emissions. CO_2 emissions are slightly lower in this scenario due to more buffering from benthic TA release. Yet, integrated over the 10 years, the total CO_2 fluxes in both model scenarios differ by < 1 %.

These initial results show that scraping of the surface sediment in the net area by ground ropes and rollers hanging between the otter boards has a demonstrable impact on enhancing atmospheric CO_2 emissions at the study site. However, this is almost entirely driven by pyrite oxidation, as shown previously for the Kiel Bight (Kalapurakkal et al., 2025). Lower measured surface pyrite contents in the HI versus CL tentatively fit with this finding. The observed decrease in benthic alkalinity fluxes by net scraping provides a very small additional weakening of the shelf carbon pump. Consequently, whilst the physical destruction of the sediment surface and enhanced pyrite oxidation are real causes for environmental concern, the additional and immediate reduction of the background alkalinity flux due to the physical removal of the surface sediment to be unimportant for the water column carbonate system. Yet, important open questions remain for further investigation, including ultimate reasons for the decline in TA and DIC fluxes observed after the trawling, the impact on aerobic versus anaerobic POC degradation, and a deeper understanding on the exact fate of resuspended sediment, including reduced iron phases.

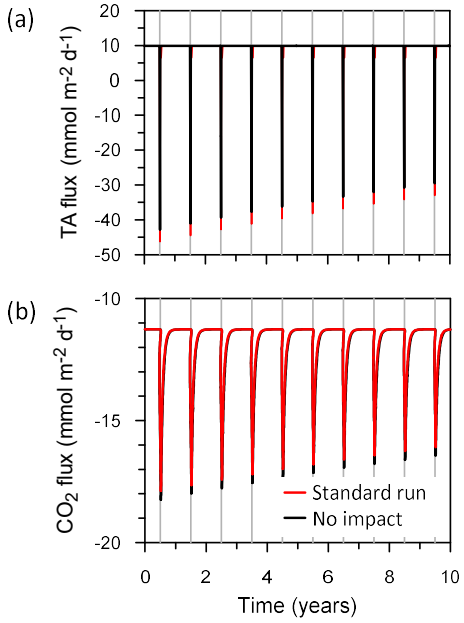

Figure 10: Results from the box model. (a) Benthic TA fluxes, and (b) CO_2 emissions to the atmosphere. The red curves show the standard model run using the observed decrease in TA and DIC fluxes following trawling, and the black curves show the fluxes without these decreases. The vertical grey lines indicate annual trawling events. Note that the red and black curves are mostly superimposed. DIC fluxes are qualitatively similar to TA fluxes (not shown).

https://doi.org/10.5194/egusphere-2025-2905
Preprint. Discussion started: 27 June 2025

5. Conclusions

This field study demonstrates that bottom trawling has a profound and lasting impact on benthic remineralization processes. Photographic evidence vividly illustrates the significant disruption to seafloor morphology, resulting in the resuspension of a sediment plume. Trawling is shown to cause substantial reductions in the fluxes of DIC, TA and nutrients in the net area, which do not fully recover to baseline levels by the end of the 16-day sampling period. The displacement of surface-active sediments directly impedes overall benthic biogeochemical processes, leading to diminished benthic fluxes and a marked reduction in the POC remineralization. Our data underscore that the diminished biological respiration, following the removal of the sediment surface, is a key driver of the reduction in DIC and TA fluxes. A coupled benthic-water column model provides insight into the broader implications of benthic TA losses for CO_2 exchange. Model results suggest that while trawling-induced reductions in TA and DIC fluxes influence carbon cycling, their impact on atmospheric CO_2 sequestration remains minor compared to trawling-induced pyrite oxidation.

To fully understand the long-term consequences of bottom trawling, further research should investigate the fate of resuspended sediments, particularly their mineralogical composition and biogeochemical reactivity. Future site-specific studies must also consider local oceanographic conditions and high-trawling-intensity areas to comprehensively assess the cumulative effects of trawling on benthic ecosystems. Such research is critical for informing sustainable fisheries management and mitigating human-induced disturbances in marine environments.

Acknowledgements

This work received funding awarded to SS and AD by the German Federal Ministry of Education and Research (BMBF), Grant No. 03F0937F, Project MGF-Ostee, DAM pilot mission: Exclusion of mobile bottom-contact fishing in marine protected areas of the German EEZ of the North Sea and Baltic Sea (MGF North Sea and MGF Baltic Sea). We thank Bettina Domeyer, Regina Surberg, Anke Bleyer, and Frauke Langenberg for assistance during the collection and analysis of sediment samples, and Matthias Türk and Asmus Petersen, and Alexandra Subic for gear preparation and deployments. We are also grateful to Gabriel Nolte, Jens Greinert and Martin Pieper for assistance with the XOFOS. The captain and crew of RV Alkor are warmly thanked for their professional and easy-going work environment on board.

Competing interests: The authors declare that they have no conflict of interest.

Author Contributions: S.S. and A.W.D. were responsible for planning and executing the study, as well as funding acquisition. S.S. conducted the BIGO and XOFOS deployments. P. L., H.T.K., and A.W.D. were involved in sediment sampling and analysis. A.W.D. conducted the modeling work. J.K. and S.B. carried out the sulfate reduction measurements, while F.S. performed the pyrite measurements. P. L., A.W.D., and S.S. prepared the manuscript with contributions from all authors.

References

Allen, J. and Clarke, K.: Effects of demersal trawling on ecosystem functioning in the North Sea: a modelling study, Mar. Ecol. Prog. Ser., 336, 63–75, https://doi.org/10.3354/meps336063, 2007.

Aller, R. C., Blair, N. E., Xia, Q., and Rude, P. D.: Remineralization rates, recycling, and storage of carbon in Amazon shelf sediments, Cont. Shelf Res., 16, 753–786, https://doi.org/10.1016/0278-4343(95)00046-1, 1996.

Almroth-Rosell, E., Tengberg, A., Andersson, S., Apler, A., and Hall, P. O. J.: Effects of simulated natural and massive resuspension on benthic oxygen, nutrient and dissolved inorganic carbon fluxes in Loch Creran, Scotland, J. Sea Res., 72, 38–48, https://doi.org/10.1016/j.seares.2012.04.012, 2012.

Apell, J. N., Shull, D. H., Hoyt, A. M., and Gschwend, P. M.: Investigating the Effect of Bioirrigation on In Situ Porewater Concentrations and Fluxes of Polychlorinated Biphenyls Using Passive Samplers, Environ. Sci. Technol., 52, 4565–4573, https://doi.org/10.1021/acs.est.7b05809, 2018.

https://doi.org/10.5194/egusphere-2025-2905
Preprint. Discussion started: 27 June 2025

Arnosti, C. and Holmer, M.: Carbon cycling in a continental margin sediment: contrasts between organic matter characteristics and remineralization rates and pathways, Estuar. Coast. Shelf Sci., 58, 197–208, https://doi.org/10.1016/S0272-7714(03)00077-5, 2003.

Atwood, T. B., Romanou, A., DeVries, T., Lerner, P. E., Mayorga, J. S., Bradley, D., Cabral, R. B., Schmidt, G. A., and Sala, E.: Atmospheric CO2 emissions and ocean acidification from bottom-trawling, Front. Mar. Sci., 10, 1125137, https://doi.org/10.3389/fmars.2023.1125137, 2024.

Bergman, M.: Mortality in megafaunal benthic populations caused by trawl fisheries on the Dutch continental shelf in the North Sea in 1994, ICES J. Mar. Sci., 57, 1321–1331, https://doi.org/10.1006/jmsc.2000.0917, 2000.

Bergman, M. J. N. and Meesters, E. H.: First indications for reduced mortality of non-target invertebrate benthic megafauna after pulse beam trawling, ICES J. Mar. Sci., 77, 846–857, https://doi.org/10.1093/icesjms/fsz250, 2020.

Boudreau, B. P.: Diagenetic models and their implementation, Springer Berlin, 1997.

Bouldin, D. R.: Models for Describing the Diffusion of Oxygen and Other Mobile Constituents Across the Mud-Water Interface, J. Ecol., 56, 77, https://doi.org/10.2307/2258068, 1968.

Bradshaw, C., Jakobsson, M., Brüchert, V., Bonaglia, S., Mörth, C.-M., Muchowski, J., Stranne, C., and Sköld, M.: Physical Disturbance by Bottom Trawling Suspends Particulate Matter and Alters Biogeochemical Processes on and Near the Seafloor, Front. Mar. Sci., 8, 683331, https://doi.org/10.3389/fmars.2021.683331, 2021.

Bradshaw, C., Iburg, S., Morys, C., Sköld, M., Pusceddu, A., Ennas, C., Jonsson, P., and Nascimento, F. J. A.: Effects of bottom trawling and environmental factors on benthic bacteria, meiofauna and macrofauna communities and benthic ecosystem processes, Sci. Total Environ., 921, 171076, https://doi.org/10.1016/j.scitotenv.2024.171076, 2024.

Brenner, H., Braeckman, U., Le Guitton, M., and Meysman, F. J. R.: The impact of sedimentary alkalinity release on the water column CO_2 system in the North Sea, Biogeosciences, 13, 841–863, https://doi.org/10.5194/bg-13-841-2016, 2016.

Bruns, I., Bartholomä, A., Menjua, F., and Kopf, A.: Physical impact of bottom trawling on seafloor sediments in the German North Sea, Front. Earth Sci., 11, 1233163, https://doi.org/10.3389/feart.2023.1233163, 2023.

Bunke, D., Leipe, T., Moros, M., Morys, C., Tauber, F., Virtasalo, J. J., Forster, S., and Arz, H. W.: Natural and Anthropogenic Sediment Mixing Processes in the South-Western Baltic Sea, Front. Mar. Sci., 6, 677, https://doi.org/10.3389/fmars.2019.00677, 2019.

Burdige, D. J.: Geochemistry of marine sediments, Princeton University Press, 2006.

Burdige, D. J.: Preservation of Organic Matter in Marine Sediments: Controls, Mechanisms, and an Imbalance in Sediment Organic Carbon Budgets?, Chem. Rev., 107, 467–485, https://doi.org/10.1021/cr050347q, 2007.

Burdige, D. J. and Komada, T.: Anaerobic oxidation of methane and the stoichiometry of remineralization processes in continental margin sediments, Limnol. Oceanogr., 56, 1781–1796, https://doi.org/10.4319/lo.2011.56.5.1781, 2011.

Burt, W. J., Thomas, H., Hagens, M., Pätsch, J., Clargo, N. M., Salt, L. A., Winde, V., and Böttcher, M. E.: Carbon sources in the North Sea evaluated by means of radium and stable carbon isotope tracers: Tracing Carbon with Ra and δ^{13} C_{DIC}, Limnol. Oceanogr., 61, 666–683, https://doi.org/10.1002/lno.10243, 2016.

Cai, W.-J. and Reimers, C. E.: Benthic oxygen flux, bottom water oxygen concentration and core top organic carbon content in the deep northeast Pacific Ocean, Deep Sea Res. Part Oceanogr. Res. Pap., 42, 1681–1699, https://doi.org/10.1016/0967-0637(95)00073-F, 1995.

https://doi.org/10.5194/egusphere-2025-2905
Preprint. Discussion started: 27 June 2025

Canfield, D. E., Raiswell, R., Westrich, J. T., Reaves, C. M., and Berner, R. A.: The use of chromium reduction in the analysis of reduced inorganic sulfur in sediments and shales, Chem. Geol., 54, 149–155, 1986.

Cline, J. D.: Spectrophotometric determination of hydrogen sulfide in natural waters 1, Limnol. Oceanogr., 14, 454–458, 1969.

Corell, H., Bradshaw, C., and Sköld, M.: Sediment suspended by bottom trawling can reduce reproductive success in a broadcast spawning fish, Estuar. Coast. Shelf Sci., 282, 108232, https://doi.org/10.1016/j.ecss.2023.108232, 2023.

Dale, A. W., Sommer, S., Ryabenko, E., Noffke, A., Bohlen, L., Wallmann, K., Stolpovsky, K., Greinert, J., and Pfannkuche, O.: Benthic nitrogen fluxes and fractionation of nitrate in the Mauritanian oxygen minimum zone (Eastern Tropical North Atlantic), Geochim. Cosmochim. Acta, 134, 234–256, https://doi.org/10.1016/j.gca.2014.02.026, 2014.

Dale, A. W., Sommer, S., Lichtschlag, A., Koopmans, D., Haeckel, M., Kossel, E., Deusner, C., Linke, P., Scholten, J., Wallmann, K., Van Erk, M. R., Gros, J., Scholz, F., and Schmidt, M.: Defining a biogeochemical baseline for sediments at Carbon Capture and Storage (CCS) sites: An example from the North Sea (Goldeneye), Int. J. Greenh. Gas Control, 106, 103265, https://doi.org/10.1016/j.ijggc.2021.103265, 2021a.

Dale, A. W., Paul, K. M., Clemens, D., Scholz, F., Schroller-Lomnitz, U., Wallmann, K., Geilert, S., Hensen, C., Plass, A., Liebetrau, V., Grasse, P., and Sommer, S.: Recycling and Burial of Biogenic Silica in an Open Margin Oxygen Minimum Zone, Glob. Biogeochem. Cycles, 35, e2020GB006583, https://doi.org/10.1029/2020GB006583, 2021b.

Dale, A. W., Geilert, S., Diercks, I., Fuhr, M., Perner, M., Scholz, F., and Wallmann, K.: Seafloor alkalinity enhancement as a carbon dioxide removal strategy in the Baltic Sea, Commun. Earth Environ., 5, 452, https://doi.org/10.1038/s43247-024-01569-3, 2024.

Dauwe, B. and Middelburg, J. J.: Amino acids and hexosamines as indicators of organic matter degradation state inNorth Sea sediments, Limnol. Oceanogr., 43, 782–798, https://doi.org/10.4319/lo.1998.43.5.0782, 1998.

Dauwe, B., Middelburg, J., and Herman, P.: Effect of oxygen on the degradability of organic matter in subtidal and intertidal sediments of the North Sea area, Mar. Ecol. Prog. Ser., 215, 13–22, https://doi.org/10.3354/meps215013, 2001.

De Borger, E., Tiano, J., Braeckman, U., Rijnsdorp, A. D., and Soetaert, K.: Impact of bottom trawling on sediment biogeochemistry: a modelling approach, Biogeosciences, 18, 2539–2557, https://doi.org/10.5194/bg-18-2539-2021, 2021.

DeMaster, D.: The diagenesis of biogenic silica: chemical transformations occurring in the water column, seabed, and crust, Treatise Geochem., 7, 407, https://doi.org/10.1016/B0-08-043751-6/07095-X, 2003.

Depestele, J., Degrendele, K., Esmaeili, M., Ivanović, A., Kröger, S., O'Neill, F. G., Parker, R., Polet, H., Roche, M., Teal, L. R., Vanelslander, B., and Rijnsdorp, A. D.: Comparison of mechanical disturbance in soft sediments due to tickler-chain SumWing trawl vs. electro-fitted PulseWing trawl, ICES J. Mar. Sci., 76, 312–329, https://doi.org/10.1093/icesjms/fsy124, 2019.

Díaz-Mendoza, G. A., Krämer, K., Von Rönn, G. A., Heinrich, C., Schwarzer, K., Reimers, H.-C., and Winter, C.: Hotspots of human impact on the seafloor in the Southwestern Baltic Sea, Cont. Shelf Res., 285, 105362, https://doi.org/10.1016/j.csr.2024.105362, 2025.

Dickson, A. G.: An exact definition of total alkalinity and a procedure for the estimation of alkalinity and total inorganic carbon from titration data, Deep Sea Res. Part Oceanogr. Res. Pap., 28, 609–623, https://doi.org/10.1016/0198-0149(81)90121-7, 1981.

Dickson, A. G., Sabine, C. L., Christian, J. R., Bargeron, C. P., and North Pacific Marine Science Organization (Eds.): Guide to best practices for ocean CO2 measurements, North Pacific Marine Science Organization, Sidney, BC, 1 pp., 2007.

https://doi.org/10.5194/egusphere-2025-2905
Preprint. Discussion started: 27 June 2025

Duplisea, D. E., Jennings, S., Malcolm, S. J., Parker, R., and Sivyer, D. B.: Modelling potential impacts of bottom trawl fisheries on soft sediment biogeochemistry in the North Sea†, Geochem. Trans., 2, 112, https://doi.org/10.1186/1467-4866-2-112, 2001.

Epstein, G., Middelburg, J. J., Hawkins, J. P., Norris, C. R., and Roberts, C. M.: The impact of mobile demersal fishing on carbon storage in seabed sediments, Glob. Change Biol., 28, 2875–2894, https://doi.org/10.1111/gcb.16105, 2022.

Ferguson, A. J. P., Oakes, J., and Eyre, B. D.: Bottom trawling reduces benthic denitrification and has the potential to influence the global nitrogen cycle, Limnol. Oceanogr. Lett., 5, 237–245, https://doi.org/10.1002/lol2.10150, 2020.

Glud, R. N.: Oxygen dynamics of marine sediments, Mar. Biol. Res., 4, 243–289, https://doi.org/10.1080/17451000801888726, 2008.

Gran, G.: Determination of the Equivalence Point in Potentiometric Titrations. Part 11, Analyst, 77, 661--671, 1952.

Grasshoff, K., Kremling, K., and Ehrhardt, M.: Methods of seawater analysis, John Wiley & Sons, 1999.

Haffert, L., Haeckel, M., Liebetrau, V., Berndt, C., Hensen, C., Nuzzo, M., Reitz, A., Scholz, F., Schönfeld, J., Perez-Garcia, C., and Weise, S. M.: Fluid evolution and authigenic mineral paragenesis related to salt diapirism – The Mercator mud volcano in the Gulf of Cadiz, Geochim. Cosmochim. Acta, 106, 261–286, https://doi.org/10.1016/j.gca.2012.12.016, 2013.

Hale, R., Godbold, J. A., Sciberras, M., Dwight, J., Wood, C., Hiddink, J. G., and Solan, M.: Mediation of macronutrients and carbon by post-disturbance shelf sea sediment communities, Biogeochemistry, 135, 121–133, https://doi.org/10.1007/s10533-017-0350-9, 2017.

Hammond, D., McManus, J., Berelson, W., Kilgore, T., and Pope, R.: Early diagenesis of organic material in equatorial Pacific sediments: stpichiometry and kinetics, Deep Sea Res. Part II Top. Stud. Oceanogr., 43, 1365–1412, 1996.

Hedges, J. I. and Keil, R. G.: Sedimentary organic matter preservation: an assessment and speculative synthesis, Mar. Chem., 49, 81–115, 1995.

HELCOM: State of the Baltic Sea--Second HELCOM holistic assessment 2011--2016, in: Baltic Sea Environment Proceedings, vol. 155, HELCOM, 2018.

Hiddink, J. G., Jennings, S., and Kaiser, M. J.: Indicators of the Ecological Impact of Bottom-Trawl Disturbance on Seabed Communities, Ecosystems, 9, 1190–1199, https://doi.org/10.1007/s10021-005-0164-9, 2006.

Hiddink, J. G., van de Velde, S. J., McConnaughey, R. A., De Borger, E., Tiano, J., Kaiser, M. J., Sweetman, A. K., and Sciberras, M.: Quantifying the carbon benefits of ending bottom trawling, Nature, 617, E1–E2, https://doi.org/10.1038/s41586-023-06014-7, 2023.

Humphreys, M. P.: Measurements and Concepts in Marine Carbonate Chemistry, University of Southampton, 2015.

Ivanović, A., Neilson, R. D., and O'Neill, F. G.: Modelling the physical impact of trawl components on the seabed and comparison with sea trials, Ocean Eng., 38, 925–933, https://doi.org/10.1016/j.oceaneng.2010.09.011, 2011.

Jorgensen, B. B.: A comparison of methods for the quantification of bacterial sulfate reduction in coastal marine sediments, Geomicrobiol. J., 1, 11–27, 1978.

Jørgensen, B. B.: Sulfur biogeochemical cycle of marine sediments, Geochem. Perspect., 10, 145–146, 2021.

https://doi.org/10.5194/egusphere-2025-2905
Preprint. Discussion started: 27 June 2025

Kaiser, M. J., Collie, J. S., Hall, S. J., Jennings, S., and Poiner, I. R.: Modification of marine habitats by trawling activities: prognosis and solutions, Fish Fish., 3, 114–136, https://doi.org/10.1046/j.1467-2979.2002.00079.x, 2002.

Kalapurakkal, H. T., Dale, A. W., Schmidt, M., Taubner, H., Scholz, F., Spiegel, T., Fuhr, M., and Wallmann, K.: Sediment resuspension in muddy sediments enhances pyrite oxidation and carbon dioxide emissions in Kiel Bight, Commun. Earth Environ., 6, 156, https://doi.org/10.1038/s43247-025-02132-4, 2025.

Kallmeyer, J., Ferdelman, T. G., Weber, A., Fossing, H., and Jørgensen, B. B.: A cold chromium distillation procedure for radiolabeled sulfide applied to sulfate reduction measurements, Limnol. Oceanogr. Methods, 2, 171–180, https://doi.org/10.4319/lom.2004.2.171, 2004.

Krumins, V., Gehlen, M., Arndt, S., Van Cappellen, P., and Regnier, P.: Dissolved inorganic carbon and alkalinity fluxes from coastal marine sediments: model estimates for different shelf environments and sensitivity to global change, Biogeosciences, 10, 371–398, https://doi.org/10.5194/bg-10-371-2013, 2013.

LaRowe, D. E., Arndt, S., Bradley, J. A., Burwicz, E., Dale, A. W., and Amend, J. P.: Organic carbon and microbial activity in marine sediments on a global scale throughout the Quaternary, Geochim. Cosmochim. Acta, 286, 227–247, https://doi.org/10.1016/j.gca.2020.07.017, 2020.

Martín, J., Puig, P., Masqué, P., Palanques, A., and Sánchez-Gómez, A.: Impact of Bottom Trawling on Deep-Sea Sediment Properties along the Flanks of a Submarine Canyon, PLoS ONE, 9, e104536, https://doi.org/10.1371/journal.pone.0104536, 2014.

Middelburg, J. J. and Levin, L. A.: Coastal hypoxia and sediment biogeochemistry, Biogeosciences, 6, 1273–1293, 2009.

Middelburg, J. J., Soetaert, K., and Hagens, M.: Ocean Alkalinity, Buffering and Biogeochemical Processes, Rev. Geophys., 58, e2019RG000681, https://doi.org/10.1029/2019RG000681, 2020.

Morys, C., Brüchert, V., and Bradshaw, C.: Impacts of bottom trawling on benthic biogeochemistry in muddy sediments: Removal of surface sediment using an experimental field study, Mar. Environ. Res., 169, 105384, https://doi.org/10.1016/j.marenvres.2021.105384, 2021.

Oberle, F. K. J., Swarzenski, P. W., Reddy, C. M., Nelson, R. K., Baasch, B., and Hanebuth, T. J. J.: Deciphering the lithological consequences of bottom trawling to sedimentary habitats on the shelf, J. Mar. Syst., 159, 120–131, https://doi.org/10.1016/j.jmarsys.2015.12.008, 2016a.

Oberle, F. K. J., Storlazzi, C. D., and Hanebuth, T. J. J.: What a drag: Quantifying the global impact of chronic bottom trawling on continental shelf sediment, J. Mar. Syst., 159, 109–119, https://doi.org/10.1016/j.jmarsys.2015.12.007, 2016b.

Olsgard, F., Schaanning, M. T., Widdicombe, S., Kendall, M. A., and Austen, M. C.: Effects of bottom trawling on ecosystem functioning, J. Exp. Mar. Biol. Ecol., 366, 123–133, https://doi.org/10.1016/j.jembe.2008.07.036, 2008.

Palanques, A., Puig, P., Guillén, J., Demestre, M., and Martín, J.: Effects of bottom trawling on the Ebro continental shelf sedimentary system (NW Mediterranean), Cont. Shelf Res., 72, 83–98, https://doi.org/10.1016/j.csr.2013.10.008, 2014.

Porz, L., Zhang, W., and Schrum, C.: Natural and anthropogenic influences on the development of mud depocenters in the southwestern Baltic Sea, Oceanologia, 65, 182–193, https://doi.org/10.1016/j.oceano.2022.03.005, 2023.

Pusceddu, A., Bianchelli, S., Martín, J., Puig, P., Palanques, A., Masqué, P., and Danovaro, R.: Chronic and intensive bottom trawling impairs deep-sea biodiversity and ecosystem functioning, Proc. Natl. Acad. Sci., 111, 8861–8866, https://doi.org/10.1073/pnas.1405454111, 2014.

https://doi.org/10.5194/egusphere-2025-2905
Preprint. Discussion started: 27 June 2025

Rabouille, C., Gaillard, J.-F., Tréguer, P., and Vincendeau, M.-A.: Biogenic silica recycling in surficial sediments across the Polar Front of the Southern Ocean (Indian Sector), Deep Sea Res. Part II Top. Stud. Oceanogr., 44, 1151–1176, https://doi.org/10.1016/S0967-0645(96)00108-7, 1997.

Rooze, J., Zeller, M. A., Gogina, M., Roeser, P., Kallmeyer, J., Schönke, M., Radtke, H., and Böttcher, M. E.: Bottom-trawling signals lost in sediment: A combined biogeochemical and modeling approach to early diagenesis in a perturbed coastal area of the southern Baltic Sea, Sci. Total Environ., 906, 167551, https://doi.org/10.1016/j.scitotenv.2023.167551, 2024.

Sala, E., Mayorga, J., Bradley, D., Cabral, R. B., Atwood, T. B., Auber, A., Cheung, W., Costello, C., Ferretti, F., Friedlander, A. M., Gaines, S. D., Garilao, C., Goodell, W., Halpern, B. S., Hinson, A., Kaschner, K., Kesner-Reyes, K., Leprieur, F., McGowan, J., Morgan, L. E., Mouillot, D., Palacios-Abrantes, J., Possingham, H. P., Rechberger, K. D., Worm, B., and Lubchenco, J.: Protecting the global ocean for biodiversity, food and climate, Nature, 592, 397–402, https://doi.org/10.1038/s41586-021-03371-z, 2021.

Schönke, M., Clemens, D., and Feldens, P.: Quantifying the Physical Impact of Bottom Trawling Based on High-Resolution Bathymetric Data, Remote Sens., 14, 2782, https://doi.org/10.3390/rs14122782, 2022.

Schroller-Lomnitz, U., Hensen, C., Dale, A. W., Scholz, F., Clemens, D., Sommer, S., Noffke, A., and Wallmann, K.: Dissolved benthic phosphate, iron and carbon fluxes in the Mauritanian upwelling system and implications for ongoing deoxygenation, Deep Sea Res. Part Oceanogr. Res. Pap., 143, 70–84, https://doi.org/10.1016/j.dsr.2018.11.008, 2019.

Sciberras, M., Parker, R., Powell, C., Robertson, C., Kröger, S., Bolam, S., and Geert Hiddink, J.: Impacts of bottom fishing on the sediment infaunal community and biogeochemistry of cohesive and non-cohesive sediments: Trawling impacts on ecosystem processes, Limnol. Oceanogr., 61, 2076–2089, https://doi.org/10.1002/lno.10354, 2016.

Slomp, C. P., Van Der Gaast, S. J., and Van Raaphorst, W.: Phosphorus binding by poorly crystalline iron oxides in North Sea sediments, Mar. Chem., 52, 55–73, https://doi.org/10.1016/0304-4203(95)00078-X, 1996.

Sommer, S., Linke, P., Pfannkuche, O., Schleicher, T., Schneider V. D, D., Reitz, A., Haeckel, M., Flögel, S., and Hensen, C.: Seabed methane emissions and the habitat of frenulate tubeworms on the Captain Arutyunov mud volcano (Gulf of Cadiz), Mar. Ecol. Prog. Ser., 382, 69–86, https://doi.org/10.3354/meps07956, 2009.

Sommer, S., Gier, J., Treude, T., Lomnitz, U., Dengler, M., Cardich, J., and Dale, A. W.: Depletion of oxygen, nitrate and nitrite in the Peruvian oxygen minimum zone cause an imbalance of benthic nitrogen fluxes, Deep Sea Res. Part Oceanogr. Res. Pap., 112, 113–122, https://doi.org/10.1016/j.dsr.2016.03.001, 2016.

Sommer, S., Dale, A. W., Bernsee, S., Domeyer, B., Gabriel, N., Kitte, A., Pankan, L., Okolski, S., Petersen, A., Subic, A., Kalapurakkal, H., and Türk, M.: Field-experiment to determine the short-term impact of bottom trawling on the benthic ecosystem in the German coastal Baltic Sea - Cruise No. AL616, 18.07. – 09.08.2024, Kiel (Germany) – Kiel (Germany), MGF-OSTSEE-2024, GEOMAR, 2025.

Stephens, J. D. and McConnaughey, R. A.: Physical and geochemical responses to bottom trawling on naturally disturbed sediments in the eastern Bering Sea, ICES J. Mar. Sci., 81, 1512–1520, https://doi.org/10.1093/icesjms/fsae094, 2024.

Tengberg, A., F De Bovee, P Hall, Berelson, W., Chadwick, D., Ciceri, G., Crassous, P., Devol, A., Emerson, S., Gage, J., Glud, R., Graziottini, F., Gundersen, J., Hammond, D., Helder, W., Hinga, K., Holby, O., Jahnke, R., Khripounoff, A., Lieberman, S., Nuppenau, V., Pfannkuche, O., Reimers, C., Rowe, G., Sahami, A., and Sayles, F.: Benthic chamber and profiling landers in oceanography — A review of design, technical solutions and functioning, Prog. Oceanogr., 35, 253–294, 1995.

Tiano, J., De Borger, E., Paradis, S., Bradshaw, C., Morys, C., Pusceddu, A., Ennas, C., Soetaert, K., Puig, P., Masqué, P., and Sciberras, M.: Global meta-analysis of demersal fishing impacts on organic carbon and associated biogeochemistry, Fish Fish., 25, 936–950, https://doi.org/10.1111/faf.12855, 2024.

https://doi.org/10.5194/egusphere-2025-2905
Preprint. Discussion started: 27 June 2025

Tiano, J. C., Witbaard, R., Bergman, M. J. N., Van Rijswijk, P., Tramper, A., Van Oevelen, D., and Soetaert, K.: Acute impacts of bottom trawl gears on benthic metabolism and nutrient cycling, ICES J. Mar. Sci., 76, 1917–1930, https://doi.org/10.1093/icesjms/fsz060, 2019.

Tiano, J. C., Depestele, J., Van Hoey, G., Fernandes, J., Van Rijswijk, P., and Soetaert, K.: Trawling effects on biogeochemical processes are mediated by fauna in high-energy biogenic-reef-inhabited coastal sediments, Biogeosciences, 19, 2583–2598, https://doi.org/10.5194/bg-19-2583-2022, 2022.

Tréguer, P. J. and De La Rocha, C. L.: The World Ocean Silica Cycle, Annu. Rev. Mar. Sci., 5, 477–501, https://doi.org/10.1146/annurev-marine-121211-172346, 2013.

Van Dam, B., Lehmann, N., Zeller, M. A., Neumann, A., Pröfrock, D., Lipka, M., Thomas, H., and Böttcher, M. E.: Benthic alkalinity fluxes from coastal sediments of the Baltic and North seas: comparing approaches and identifying knowledge gaps, Biogeosciences, 19, 3775–3789, https://doi.org/10.5194/bg-19-3775-2022, 2022.

Van Denderen, P. D., Bolam, S. G., Friedland, R., Hiddink, J. G., Norén, K., Rijnsdorp, A. D., Sköld, M., Törnroos, A., Virtanen, E. A., and Valanko, S.: Evaluating impacts of bottom trawling and hypoxia on benthic communities at the local, habitat, and regional scale using a modelling approach, ICES J. Mar. Sci., 77, 278–289, https://doi.org/10.1093/icesjms/fsz219, 2020.

van de Velde, S., Van Lancker, V., Hidalgo-Martinez, S., Berelson, W. M., and Meysman, F. J. R.: Anthropogenic disturbance keeps the coastal seafloor biogeochemistry in a transient state, Sci. Rep., 8, 5582, https://doi.org/10.1038/s41598-018-23925-y, 2018.

Wallmann, K., Diesing, M., Scholz, F., Rehder, G., Dale, A. W., Fuhr, M., and Suess, E.: Erosion of carbonate-bearing sedimentary rocks may close the alkalinity budget of the Baltic Sea and support atmospheric CO2 uptake in coastal seas, Front. Mar. Sci., 9, 968069, https://doi.org/10.3389/fmars.2022.968069, 2022.

Watling, L., Findlay, R. H., Mayer, L. M., and Schick, D. F.: Impact of a scallop drag on the sediment chemistry, microbiota, and faunal assemblages of a shallow subtidal marine benthic community, J. Sea Res., 46, 309–324, https://doi.org/10.1016/S1385-1101(01)00083-1, 2001.

Yuan-Hui, Li and Gregory, Sandra: Diffusion of ions in sea water and in deep-sea sediments, Geochim. Cosmochim. Acta, 38, 703–714, 1974.

Zeebe, R. E. and Wolf-Gladrow, D.: CO2 in seawater: equilibrium, kinetics, isotopes, Elsevier, 2001.

Zhang, W., Porz, L., Yilmaz, R., Wallmann, K., Spiegel, T., Neumann, A., Holtappels, M., Kasten, S., Kuhlmann, J., Ziebarth, N., Taylor, B., Ho-Hagemann, H. T. M., Bockelmann, F.-D., Daewel, U., Bernhardt, L., and Schrum, C.: Long-term carbon storage in shelf sea sediments reduced by intensive bottom trawling, Nat. Geosci., 17, 1268–1276, https://doi.org/10.1038/s41561-024-01581-4, 2024.